HAL
open science

Insight into shell growth dynamics of Mactromeris polynyma in the St. Lawrence Estuary using sclerochemistry

Justine Doré, Julien Thébault, Virginie Roy, Fabien Dewilde, Gwénaëlle Chaillou

To cite this version:

Justine Doré, Julien Thébault, Virginie Roy, Fabien Dewilde, Gwénaëlle Chaillou. Insight into shell growth dynamics of Mactromeris polynyma in the St. Lawrence Estuary using sclerochemistry. Marine Chemistry, 2021, 234, pp.103987. 10.1016/j.marchem.2021.103987 . hal-04211562

HAL Id: hal-04211562

https://hal.science/hal-04211562

Submitted on 19 Sep 2023

HAL is a multi-disciplinary open access archive for the deposit and dissemination of scientific research documents, whether they are published or not. The documents may come from teaching and research institutions in France or abroad, or from public or private research centers.

L'archive ouverte pluridisciplinaire **HAL**, est destinée au dépôt et à la diffusion de documents scientifiques de niveau recherche, publiés ou non, émanant des établissements d'enseignement et de recherche français ou étrangers, des laboratoires publics ou privés.

Version of Record: https://www.sciencedirect.com/science/article/pii/S0304420321000724
Manuscript_e0b0aa85045bb24ecdef12cdad86b9d1

Insight into shell growth dynamics of *Mactromeris polynyma* in the St. Lawrence Estuary using sclerochemistry

Justine **Doré**[1*], Julien **Thébault**[1], Virginie **Roy**[2], Fabien **Dewilde**[3], Gwénaëlle **Chaillou**[4*]

[1] Univ Brest, CNRS, IRD, Ifremer, LEMAR, Plouzané, 29280, France

[2] Maurice Lamontagne Institute, Fisheries and Oceans Canada, 850 route de la Mer, C.P. 1000, Mont-Joli, QC, G5H 3Z4, Canada

[3] Univ Brest, CNRS UMS3113, Plouzané, 29280, France

[4] Canada Research Chair in Geochemistry of Coastal Hydrogeosystems, Québec-Océan, ISMER, UQAR, Rimouski, QC, G5L 3A1 Canada

[*] Correspondence: Justine Doré, justine.dore91@gmail.com

[*] Correspondence: Julien Thébault, julien.thebault@univ-brest.fr

© 2021 published by Elsevier. This manuscript is made available under the Elsevier user license
https://www.elsevier.com/open-access/userlicense/1.0/

Keywords:

Mactromeris polynyma; chemochronology; growth; Lower St. Lawrence Estuary

Abstract:

This study explores the potential of geochemical data to accurately date *Mactromeris polynyma* shells collected in the Lower St. Lawrence Estuary, and to assess the species' utility as an environmental archive. Previous growth studies of *M. polynyma* from the St. Lawrence ecosystem showed a possible overestimation of annual growth lines using the classic sclerochronology methodology. Our study proposes a new method based on chemochronology, coupling Ba/Ca and Sr/Ca ratio profiles to distinguish between disturbance lines and actual annual growth lines. By aligning the Sr/Ca profiles thanks to the peaks of Ba/Ca, drastic decreases in the Sr/Ca ratio have been highlighted. These drops, which are detectable in all specimens, precisely locate the annual growth lines, making it possible to study variations in the growth rate. Our chemochronology method is a powerful tool for precisely aging *M. polynyma*, making this innovative method an alternative to sclerochronology techniques for highlighting annual growth lines for species that are difficult to age.

Highlights:

Chemochronology as a new methodology to age specimens

Ba/Ca ratio as a tool to align Sr/Ca ratio profiles

Aligned Sr/Ca ratio profiles show common sharp decreases among specimens

Sharp Sr/Ca ratio decreases accurately locate annual growth lines

M. polynyma has great potential as an environmental archive

1. Introduction

Biogeochemical archives such as sediment cores, coral skeletons, otoliths, or mollusk shells act as recorders of their surrounding medium and provide evidence of past environmental conditions when specific environmental proxies are developed. Freshwater and marine bivalves can furnish life-history information, such as a continuous record of their growth and environmental changes in the ambient water (Rhoads and Lutz, 1980; Rosenberg and Runcorn, 1975). Because many bivalve species are extremely long-lived, non-colonial animals (some living to >500 years; Butler et al., 2013; Strom et al., 2004; Thompson et al., 1980; Wanamaker et al., 2008), they are valuable in paleoclimate (e.g., Butler et al., 2010; Scourse et al., 2006), water quality (e.g., Black et al., 2017; Dunca et al., 2005; Gillikin et al., 2005), and age (e.g., Abele et al., 2009; Kilada et al., 2007, 2009) studies. Moreover, due to their vast biogeographic distribution and long geologic history (i.e., abundant fossils are present for the past ca. 500 million years), bivalves can provide environmental data from many different settings over millions of years (see Richardson, 2001, for a review).

Bivalve shells grow by accretion of calcium carbonate crystals and form growth increments throughout ontogeny. Growth rate varies in response to changes in local and regional environmental conditions and/or biologic events, like spawning (Jones et al., 1983). Growth can stop at several periodicities, including ultradian, circatidal, circalunidian, fortnight, month, or annual time scales (Schöne, 2008), this cessation of growth form the so-called growth lines. Thus, bivalves act as a calendar, providing precise dates of high-resolution climate records and environment changes. The aim of sclerochronology is to date bivalves (and other calcium carbonate secreting organisms) by extracting these growth patterns (see Schöne and Surge, 2012, for a review) in order to reconstruct past environmental conditions.

The St. Lawrence marine ecosystem (i.e., Estuary and Gulf) is one of the largest and most productive estuarine–marine ecosystems in the world (Gilbert and Dufour, 2008). It is also a complex coastal system (Lavoie et al., 2007; Savenkoff et al., 2007) that receives more than half of the freshwater inputs from eastern North America (Dufour and Ouellet, 2007). Due to human uses and pressures in

the Great Lakes Basin, freshwater as well as nutrient, organic matter, and contaminant inputs are leading to important changes in the Lower St. Lawrence Estuary and Gulf (EGSL), including hypoxia and acidification of deep bottom waters in the Laurentian Channel (Gilbert et al., 2005, 2007; Mucci et al., 2011; Jutras et al., 2020). Over the last 20 years, some studies have focussed on the sediment records along the hypoxic gradient, including both foraminifera (Genovesi et al., 2011; Thibodeau et al., 2006) and redox-sensitive trace metals (Lefort et al., 2012). Moreover, the Atlantic Zone Monitoring Program (AZMP), implemented since 1998 by Fisheries and Oceans Canada (DFO), has characterized the oceanic variability of the system at seasonal, inter-annual, and decadal scales (e.g., Blais et al., 2019; Galbraith et al., 2019). However, these studies mostly concentrate on the deep Laurentian Channel, while data from coastal areas along the St. Lawrence shores are still sparse except in some harbours (e.g., Degtlareva and Elektorowicz, 2001; Dutil et al., 2012). As far as we know, no studies have yet used mollusk sclerochronology to assess coastal environmental changes over time along the St. Lawrence shores, although the St. Lawrence coastal ecosystem has numerous bivalve species, such as the Arctic Surfclam *Mactromeris polynyma,* that could provide useful information on coastal environment changes (Bourdages et al., 2012).

In the last three decades, DFO scientific missions have discovered numerous mollusk beds along eastern Canadian coasts (i.e., North Shore of the St. Lawrence Estuary and Gulf, the Îles-de-la-Madeleine in the southwestern Gulf of St. Lawrence, Scotian Shelf, Grand Banks) that revealed *M. polynyma* to be a commonly distributed and abundant coastal species (Brulotte, 1995; Cyr, 1994; DFO, 2006; Lambert and Giguère, 1994; Lambert and Goudreau, 1995a; Landry et al., 1992a). *M. polynyma* is known to be a sedentary endobenthic bivalve mollusk forming beds in sublittoral zones or under the low tide line. They are found buried in sandy sediments (Bourassa et al., 2008; Lambert and Goudreau, 1995b) at depths determined by the length of their siphons and consequently their size (e.g., adult surf clams can reach 150 mm in length). They feed by using their incurrent siphon to filter suspended materials. In the St. Lawrence Estuary and Gulf, Arctic Surfclams can be found at water depths ranging from 1 to 60 m, with a maximum density observed between 15 and 20 m in depth (Trottier and Goudreau, 2015). Due to its biological and ecological characteristics, *M. polynyma* could

be a valuable asset for sclerochronology and sclerochemistry studies (Mann et al., 2013) in the coastal EGSL and more generally in arctic and subarctic regions, where fisheries and economic interests are increasing (DFO, 2018). Several fisheries management reports describe *M. polynyma* as a slow-growing, long-living species (i.e., it would take 13 to 20 years to reach 80 mm in length, depending on the fishing bed) (Bourassa et al., 2008; Lambert and Goudreau, 1999; Landry et al., 1992b; Roddick et al., 2012).

To reconstruct past environmental variations, associating a specific date of formation to a given shell portion is the first step in defining a timeline for proxies that are contained in growth rate (i.e., growth anomalies) and embedded in the carbonate shell material (i.e., geochemical variations) (e.g., Fenger et al., 2007; Hudson et al., 1976; Schöne et al., 2013; Strom et al., 2004). However, accurate age determination in long-living bivalve shells is not always straightforward because of uncertainties in locating growth lines on the external or internal shell. The determination of accurate annual growth lines depends on many interrelated variables. There are several sources of bias when using sclerochronology to identify growth lines: tools that emphasize growth lines (e.g., blue light excitation: Wanamaker et al., 2009; Mutvei's solution: Schöne et al., 2005), microscope type and magnification (e.g., digital microscope with 10x or 500x magnification), and the operator. In the case of *M. polynyma*, several technical reports (government of Canada publications) have revealed a bias in the growth estimates of specimens collected around the Gulf of St. Lawrence when counting lines on the external shell due to excessive number of lines (Lambert and Goudreau, 1997, 1999). Other reports on the growth rate of *M. polynyma* in the EGSL based their assess on the inside of a hinge plate cut out of the shell where excessive growth lines make visual counting difficult too (Bourassa et al., 2008; Roddick et al., 2012). In both case, the authors pointed out the difficulty to assess accurate ages with this species making the use of cross-dating method unenforceable despite its practice recommended in sclerochronology (e.g., Griffin, 2012). Thus, we highlight the necessity to use geochemical technique to counterbalance this issue.

An accurate localization of annual growth lines is essential to determine age and growth rate because individuals may form growth lines at different periodicities and even when they are stressed, making

localization much more difficult. On a time scale ranging from a few years to several decades, no study has shown any alteration in the geochemical composition of the shells after biomineralization (e.g., Schöne, 2013, Walliser et al., 2015). Thus, geochemical approaches could be used to determine the age of bivalve species with indistinct growth lines (e.g., Cardoso et al., 2013a; Gurney et al., 2005; Kilada et al., 2009; Richardson et al., 2004). Geochemical methods provide an additional tool to age shells while reducing reading errors with misidentifying growth lines. Such methods may be used on *M. polynyma* to determine annual growth lines and to test its use as an environmental archive.

Several studies have highlighted the potential of using the oxygen stable isotopic ratio ($\delta^{18}O$) and the strontium-to-calcium ratio (Sr/Ca) as tools to estimate and validate age by identifying annual growth lines of different bivalve species (e.g., Cardoso et al., 2013a, 2013b; Foster et al., 2009; Gurney et al., 2005; Witbaard et al., 1994). No consensus has yet been reached on the incorporation dependency of Sr into bivalve shells. The Sr/Ca ratio can be linked to water temperature (Richardson et al., 2004) and salinity (Dodd and Crisp, 1982) as well as metabolic activities like growth rate (Carré et al., 2006; Gillikin et al., 2005; Lorrain et al., 2005; Takesue and van Geen, 2004). In this study, the main objective is to propose a new geochemical approach as an alternative to standard sclerochronological techniques in order to build an age model for each *M. polynyma* shell, which is the first essential step for paleo-environmental studies. More specifically, we first develop a step-by-step methodology to locate annual growth lines combining synchronous patterns of trace element ratios. Secondly, we explore the growth pattern synchronicity between specimens of *M. polynyma* collected at our study site in the Lower St-Lawrence Estuary. According to our knowledge, the study is the first to combine geochemical profiles in order to age and evaluate growth rate of bivalve species with excessive disturbances lines, offering a new approach to assess the species' potential to record environmental variations.

2. Materials and sample site

The study site is located on the North Shore of the Lower St. Lawrence Estuary (LSLE, Quebec, Canada; Fig. 1), in DFO fishing area 1B, where three distinct beds of Arctic Surfclams have been identified (Fig. 1C). The sample site chosen for this study is the Baie-Comeau bed (called Baie-Comeau hereafter). *M. polynyma* shells were collected in late July 2018 at the northern edge of Baie-Comeau (49° 11′ 35.326″N – 68° 05′ 22.866″W) at 10 m depth during the DFO Maurice Lamontagne Institute's oceanographic campaign (IML-2018-029) on-board the CCGS *Leim* (Fig. 1C). The harvest was performed with a New England hydraulic dredge with jets of water at the base of the blade (pressure between 241 and 621 kPa). This technique has the advantage of softening the bottom sediment and reaching specimens buried up to 20 cm deep (DFO, 2018). Shells were collected alive and soft tissue were removed shortly after sampling. Seven shells were selected because of their size spectrum and good state of preservation (e.g., absence of holes or breaks in the shell). In this study, a restricted size range was chosen so that individuals were neither too large (i.e., potentially old, thus decreasing the analysis resolution of the last years of life) nor too small (i.e., to avoid having insufficient data) in order to facilitate geochemical analyses and data comparison between specimens.

FIGURE 1 (2 columns)

3. Methodology for the validation of annual growth lines

To explore the potential of *M. polynyma* as an environmental archive, growth lines must first be determined to age and evaluate the growth rate of each specimen prior to reconstruction of past environmental variations. However, standard sclerochronological techniques as cross-dating were not conclusive to age specimens. Thus, geochemical analyses were performed on shells to identify growth lines having an annual periodicity (called annual growth lines hereafter). The step-by-step approach is presented in Fig. 1S.

3.1. Preparation of shells

Because of external shell impurities and fragility, especially toward the ventral margin, hinge plates (HPs) were selected to study the growth of six specimens of *M. polynyma* (M07, M08, M10, M12, M14, and M15). In addition, the whole small and practically unbroken shell of one specimen (M17) was added to study the outer shell layer. Table 1 presents the morphometric features of the selected specimens. Two 1 mm thick "mirror" cross sections were cut from the six HPs and one entire shell along the axis of maximum growth, from the umbo to the ventral margin, using a low-speed precision saw (Struers, Secotom-10; rotation speed of 500 rpm; feed rate of 100 $\mu m.s^{-1}$) equipped with a 600 µm thick diamond-coated blade continuously cooled by water. Beforehand, shells had been embedded in a 1 cm wide thick layer of a quick-drying metal epoxy resin (Araldite Metal, Huntsman Advanced Materials) along the axis to protect shells from breaks during sectioning or manipulation. Each section was then glued on a glass side, ground with 1200 then 2500 grit wet table carborundum paper, and polished with 1 µm diamond liquid (ESCIL, Chassieu, France) on a polishing cloth fixed on a grinding turntable (Struers, TegraPol-25). To reduce scratches and contamination hazards, cross-sections were cleaned between each grinding/polishing step with deionized water and dried to eliminate residual diamond liquid and/or abrasive material. For each specimen, a "mirror" HP cross section was used for sclerochronological analysis whereas trace element analyses (TEA) were performed on the other HP cross section (Fig. 2). Oxygen stable isotope analyses (SIA) was only performed on the entire shell of M17 (Fig. 2).

To visually locate growth lines, digital images of all "mirror" HP cross sections were taken with a stereomicroscope (20x magnification; Zeiss Lumar.V2) and a digital microscope (500x magnification; Keyence, VHX 600), both of which were equipped with a motorized stage. For the outer shell layer (OSL), only the stereomicroscope was used. To enhance growth line readability on HPs, cross sections were immersed in Mutvei's solution for 30 min at ambient temperature (Schöne et al., 2005) and the same imaging method was applied. Images were processed with ImageJ software to attribute a distance to each growth line.

FIGURE 2 (2 columns)

TABLE 1 (1 column)

3.2. Stable isotope analysis (SIA)

The oxygen-isotope ratio ($\delta^{18}O_{shell}$) was measured in the OSL of specimen M17. This shell cross section was pre-rinsed ultrasonically with demineralized water. Discrete samples of powdered carbonate were then obtained using a computer-operated MicroMill® coupled with a 300 µm diameter drill. Short tracks about 900 µm long, 200 µm thick, and 10 µm deep (milling to 10 µm in depth allowed us to reduce the drill diameter to 200 µm) were drilled parallel to growth lines in the second half of the cross section (sampling started 7 mm from the ventral margin because of shell fragility). Consecutive tracks overlapped by at least 50 µm. These parameters allowed the sampling of ~15 µg of $CaCO_3$ with an average spatial resolution of ca. 150 µm (Fig. 2E). Isotopic analyses were performed at the Pôle Spectrométrie Océan (PSO, Plouzané, France) using a MAT-253 (Thermo Scientific) stable isotope ratio mass spectrometer (IRMS) coupled with a Kiel IV Carbonate Device (Thermo Scientific). Oxygen-isotope ratios were standardized with the VPDB scale using NBS-19 and NBS-18 international carbonate standards (Coplen, 1996). The assigned value was $\delta^{18}O_{VPDB}$ = –2.20‰ for NBS-19 and $\delta^{18}O_{VPDB}$ = -23.20‰ for NBS-18. External precision (1σ), based on repeated measurements of an in-house standard, was ± 0.04‰. Due to breaks, bioerosion, and the fragile OSL, $\delta^{18}O_{shell}$ was only measured on 22.4 mm within 7 mm of the ventral margin of the OSL, thus the date of death could not be used to determine date oscillations.

In addition to the measured $\delta^{18}O_{shell}$, we calculated a monthly theoretical shell $\delta^{18}O$ ($\delta^{18}O_{theo}$) based on mean seawater temperature and salinity data from 2010 to 2018 measured close to the sample site. The $\delta^{18}O_{theo}$ was calculated using the paleothermometry equation developed by Grossman and Ku

(1986) for biogenic aragonite and re-evaluated using the most recent $\delta^{18}O$ correction of -0.27 (Hut, 1987) shown by the equation 1:

eq. (1) $$T°C = 20.6 - 4.34\left(\delta^{18}O_{theo} - (\delta^{18}O_{sw} - 0.27)\right)$$

where $\delta^{18}O_{sw}$ was deduced from the linear regression between salinities and $\delta^{18}O_{sw}$ of the seawater measured by Tan and Strain between 1980 and 1996 (most complete and recent data) along the Estuary and Gulf of St. Lawrence (Fig. 2S) and accessible on the NOAA website (https://data.giss.nasa.gov/cgi-bin/o18data/geto18.cgi). We rewrote the paleothermometry relationship to calculate $\delta^{18}O_{theo}$ values (eq. 2):

eq. (2) $$\delta^{18}O_{theo} = \frac{19.4282 - T°C + 4.34(\delta^{18}O_{sw})}{4.34}$$

Salinities and water temperatures used to calculate $\delta^{18}O_{theo}$ are from the instrumented oceanographic buoy identified as PMZA-RIKI (48°40′01″N-68°35′11″W). This buoy is 70 km far from the sample site, but it provides the nearest oceanographic time series available. The $\delta^{18}O_{sw}$ was then written as followed:

eq. (3) $$\delta^{18}O_{sw} = 0.2859(\pm 0.015)^{*}S - 10.6997(\pm 0.35)$$

According to equation 3, a value of zero for the $\delta^{18}O_{sw}$ corresponds to an ambient salinity of 37.42. Thus, a salinity variation of 1 reflects a fluctuation of 0.285‰ in the $\delta^{18}O_{sw}$ composition. $\delta^{18}O_{sw}$ was then used in eq. (2) to accurately calculate $\delta^{18}O_{theo}$ at the location of buoy PMZA-RIKI. Then, a macroscopic comparison was done between monthly $\delta^{18}O_{theo}$ and $\delta^{18}O_{shell}$ oscillations. Extreme positive values from $\delta^{18}O_{theo}$ and $\delta^{18}O_{shell}$ (e.g. winter temperatures) were matched and they were used to validate the annual periodicity of the $\delta^{18}O_{shell}$ oscillations. The SIA points out the presence of numerous supplementary lines that are unlikely of seasonal or annual origin (Fig. 1S) and leads to the consideration of a new method for locating lines that are annual.

3.3. Trace element analysis (TEA)

Because the shell is fragile and bioerosion mechanisms may remove the first years of life, the hinge plates were used for trace element analysis (TEA). Thus, trace elements of only one OSL (M17) and the other 6 HPs (Table 1, Fig. 2) were analyzed with a Nu Attom high-resolution inductively coupled plasma mass spectrometer (HR-ICP-MS) coupled with a Photon-Machines G2 laser ablation (LA-ICP-MS) system at the Research Centre on the Dynamics of the Earth System (GEOTOP), Université du Québec à Montréal (UQAM). Several trace elements were measured, but only ^{135}Ba, ^{86}Sr, and ^{43}Ca (internal standard) are presented here. Elemental ratios (E/Ca) were obtained using IOLITE software (https://iolite-software.com/) after instrumental drift correction and normalization. Operating conditions and processes are detailed in Doré et al. (2020). Raw data were smoothed using a 10- and 100-point running mean for HP and OSL profiles, respectively.

Element-to-calcium ratio profiles (Ba/Ca and Sr/Ca) were used to quickly and accurately detect annual growth lines in HPs. The Ba/Ca ratio profiles are often characterized by a flat background interrupted by sharp peaks detectable in conspecific and contemporaneous specimens from the same locality (Carré et al., 2006; Gillikin et al., 2006; Lazareth et al., 2003; Stecher et al., 1996; Thébault et al., 2009; Vander Putten et al., 2000) and they can be used as proxy of the phytoplankton dynamics (e.g., Doré et al., 2020; Stecher et al., 1996; Thébault et al., 2009) and as cross-dating tool by aligning profiles (Doré et al., 2020; Marali et al., 2017). However, even if Ba/Ca profiles recorded on *M. polynyma* hinge plates offer some inter-annual variabilities, information on the position of annual growth lines cannot be accurately inferred from these signals. Indeed, these lines are located somewhere within the flat portions of the Ba/Ca profile. Without additional clues, their exact position cannot be identified precisely. Conversely, Sr/Ca ratio profiles are usually formed of annual oscillations that can be very useful in highlighting a sharp decrease in growth (i.e., halt in growth) due to the positive correlation between Sr/Ca and shell growth rate (Carré et al., 2006; Gillikin et al., 2005; Lorrain et al., 2005; Takesue and van Green, 2004). Therefore, Sr/Ca signals could be useful to identify with a good accuracy the position of annual growth lines. Unfortunately, in some of our

specimens, Sr/Ca annual cycles could be interrupted with one or more sharp decreases that could be misinterpreted as annual lines. In addition, the relatively high inter-individual variability prevents accurate temporal alignment of Sr/Ca profiles. This issue could be fixed by aligning Sr/Ca profiles of different specimens using the likeness of their Ba/Ca signals to highlight a similar, simultaneous, Sr/Ca decrease, which can corresponds to an annual growth line. Thus, firstly, we used the maximum value of similar Ba/Ca peaks between signals to align Ba/Ca profiles, and, secondly, each profile was re-sampled as a function of the longest distance between two consecutive peaks using a homemade script built using R software (cran.r-project.org; available on request). Finally, these resampled and synchronized signals were then used to align inter-individual Sr/Ca profiles. This alignment visually highlights common inter-individual Sr/Ca patterns, which could identify annual growth lines. The positions of annual growth lines were set in the most likely locations (i.e., when most—but not always all—locations had a common Sr/Ca ratio pattern). To validate the position of annual growth lines, we compared positions of presumed annual growth lines determined by both SIA and TEA on the OSL of specimen M17.

3.4. Growth chronology from trace element profiles

Based on the age determined by TEA, a von Bertalanffy growth function (eq. 4) was applied and fitted to the shell length-at-age data:

eq. (4) $$L_t = L_\infty\left(1 - e^{-K(t-t_0)}\right)$$

where L_t is the shell length (in mm) at time t (in years), L_∞ is the length reached after an infinite time of growth (in mm), K is the Brody growth constant defining the "speed" of growth (per year), and t_0 is the theoretical age at which the length would be zero (in years). Because only HPs were studied, the length referring to the external shell was calculated using an allometric relationship (eq. 5):

eq. (5) $$L_t = a\left(\frac{L_{OSL}}{L_{HP}}\right)$$

where a is the length of each increment measured in the HP, and L_{OSL} and L_{HP} are the total length of the shell and the HP, respectively.

In addition, the ontogenetic trend (i.e., physiological effect on growth where the older a specimen the less it grows) was mathematically removed using a negative exponential curve then a cubic spline. Growth indices (GIs) were then obtained to examine the potential of *M. polynyma* to archive environmental variations that had equal influence on growth rates. Thus, GIs (eq. 6) were calculated for each year of each specimen by dividing measured and predicted increment widths (IW):

eq. (6) $$GI_t = \frac{(IW_{measured})_t}{(IW_{predicted})_t}$$

where GI_t is the growth index at time t (in years), $IW_{measured}$ is the width of the measured annual increment at t, and $IW_{predicted}$ is the predicted increment width at t. The GIs for each time series were then standardized following eq. (7):

eq. (7) $$SGI_t = \frac{GI_t - \mu}{\sigma}$$

where μ is the average and σ the standard deviation of all GI values at time t. SGIs were estimated using the dplR package in R (https://CRAN.R-project.org/package=dplR) (Bunn, 2008). A master chronology, representing the average of SGI chronologies, was then calculated using aged shells in order to maximise the accuracy of the method (i.e., hinge plates only).

3.5. Statistical analyses

Synchrony between aligned Sr/Ca signals was tested using a pairwise matrix correlation on a common growth period. Linear regression was used to calculate the coefficient of determination and Pearson's product-moment correlation was used to determine the coefficient of correlation; both were applied to smoothed HP signals. The associated p-value was also calculated. Robustness of the master chronology was assessed through calculation of the expressed population signal (EPS) using the dplR package as follows (eq. 8):

eq. (8) $$EPS = \frac{n(R_{bar})}{(n(R_{bar})+(1-R_{bar}))}$$

where R_{bar} is the average of all correlations between pairs of SGI chronologies and n is the number of specimens used to construct the master chronology. If the EPS value is higher than the arbitrary threshold of 0.85 (Wigley et al., 1984), the variance of the estimated master chronology sufficiently expresses the variance of all SGI series.

4. Results and Discussion

4.1. A step-by-step chemochronology approach for dating specimens

Numerous growth lines are present on the OSLs and HPs of our seven *M. polynyma* specimens, and disrupt the identification of annual growth lines (Fig. 3S). If all lines were considered to be annual growth stops, our specimens would be centuries old, which is highly unlikely. Therefore, most of those excessive lines are probably so-called "disturbance" lines formed as a result of stress. The origin of this stress is unknown and could be related to predation or fishery (trawling) activity as observed for other bivalves as, for example, for *Ensis spp.* (Robinson and Richardson, 1998), *G glycymeris* (Ramsay et al., 2000) and *A islandica* (Klein and Witbaard, 1993; Witbaard and Klein, 1994). In this context, we could not visually estimate the age and growth rate of *M. polynyma* with a high level of confidence even using cross-dating method. To resolve this difficulty, we provide here an alternative step-by-step method based on geochemical ratio profiles. This chemochronology methodology allows to avoid the constraints of macroscopic observations and focuses on the geochemical content of the shells to age specimens.

4.1.1. Shell $\delta^{18}O$ and determination of annual growth lines

The oxygen-isotope ratio ($\delta^{18}O_{shell}$) was measured on 54 samples micromilled along the OSL of specimen M17. This isotopic profile showed four discernible oscillations (i.e., variation between two

accurate positive extreme values) along 22.4 mm (between 9.7 and 32.1 mm from the ventral margin; Fig. 3), ranging from –1.39 to +2.09‰ (mean = 0.30‰; s.d. = 0.92‰). These oscillations suggest a seasonality with alternatively high (corresponding to lower temperatures during winter) and low (corresponding to higher temperatures during summer) $\delta^{18}O$ values. The $\delta^{18}O_{theo}$ profile calculated based on *in situ* temperature and salinity also shows regular seasonal oscillations that range from around –1.82‰ to +3.22‰, with an average of +0.73‰ ± 0.90‰ (Fig. 3).

FIGURE 3 (2 columns)

Figure 3 shows the high overlap between $\delta^{18}O_{shell}$ and $\delta^{18}O_{theo}$ from 2013 to 2016, revealing the presence of disturbance/stress lines in addition to annual growth lines. These two oxygen-isotope ratio profiles provide a useful tool to visually eliminate non-annual growth lines and could inform on the growth cessation period. Indeed, even if global oscillation values are slightly different (because environmental data were recorded in the middle of the LSLE, approximately 70 km from Baie-Comeau), variations below 1‰ for $\delta^{18}O_{shell}$ values (higher temperature), especially in 2014 and 2015, are similar to $\delta^{18}O_{theo}$ variations. However, variations are different for values above 1‰ (lower temperature). It should be noted that $\delta^{18}O_{theo}$ values for some winter months (December to March) are lacking due to missing water temperature and salinity data during this ice-covered period. Moreover, when these values were available, we found no matches. Shells seem to stop recording variations of $\delta^{18}O$ with colder temperatures. However, as no annual growth line can be identified using only the oscillations of $\delta^{18}O$, no certainty can be advanced on the period of growth cessation at this stage of the study. Furthermore, some amount of time averaging during carbonate sampling cannot be exclude.

Investigating the age and growth rate of *M. polynyma* shells using variability $\delta^{18}O_{shell}$ could have been applied on the condition that samples were taken up to the ventral margin (known date of death). However, this study involves one major drawback: the slow shell growth rate and the relatively large diameter of the drill bit used for carbonate sampling preclude the accurate estimation of shell growth dynamics. In addition, accurate aging of shells using the OSL may be challenging due to the high risk of bioerosion, attacks of euendoliths, and potential breakage. Oxygen-isotope sampling and analysis

are also time consuming and expensive. Considering this, the use of trace elements archived in shell hinge plates may offer an efficient and low-cost alternative for determining the age of bivalve shells.

FIGURE 4 (2 columns)

4.1.2. Localization of annual growth lines using trace elements

Numerous studies have investigated variations in trace element concentrations related to biological and environmental changes in biogenic carbonate (Ballesta-Artero et al., 2018; Doré et al., 2020; Druffel, 1997; Freitas et al., 2006; Langlet et al., 2002; Lea et al., 1989; Poulain et al., 2015; Prendergast et al., 2017). Variations in Sr concentration have been related to an array of environmental or biological drivers, including water temperature, salinity, and metabolic activities such as growth rate (Dodd, 1965; Klein et al., 1996; Langlet et al., 2002; Lorrain et al., 2005; Richardson et al., 2004; Stecher et al., 1996; Wanamaker and Gillikin, 2019). Several studies related Sr/Ca ratio variations to the metabolic activity of the mantle epithelium (Carré et al., 2006; Langlet et al., 2002; Stecher et al., 1996) and/or to shell growth rate (Cardoso et al., 2013a; Carré et al., 2006; Pearce and Mann, 2006; Stecher et al., 1996).

In our study, the similarity (size and occurrence) of Ba/Ca peaks between specimens (Fig. 4) was used to align inter-specimen Sr/Ca profiles, since this signal does not give information on the position of annual growth lines. In this way, a comparison between different Sr/Ca ratio profiles (i.e., from several *M. polynyma* specimens) aligned using Ba/Ca peaks would help to locate sharp and synchronous decreases in Sr/Ca profiles, similar to how cross-dating techniques are applied to reveal growth lines.. After alignment, profiles show highly synchronized sharp Sr/Ca ratio decreases (Fig. 5) among the six HPs, even though all profiles were only slightly, but significantly, correlated (average r = 0.38; p-value < 0.001; Table 2). Previous studies considered that lower Sr incorporation was linked to a decrease of growth rate (or cessation, forming a growth line) (e.g., Carré et al., 2006 for *Mesodesma donacium* and *Chione subrugosa;* Stecher et al., 1996 for *Spisula solidissima*). Therefore,

the common Sr/Ca decreases that we observed here indicate, with a high degree of confidence, the positions of annual growth lines.

FIGURE 5 (2 columns)

TABLE 2 (1 column)

4.1.3. Validation of the chemochronology methodology with determination of age and growth patterns

Figure 6 shows decreases in the Sr/Ca ratios, for M10 specimen as an example. The decreases coincide with the growth line positions on the "mirror" HP and, therefore, locate accurate annual growth lines. The annual portions of Ba/Ca ratio profiles delimited by these annual growth lines are also similar to portions of the Ba/Ca profile measured in the OSL as highlight by oxygen-isotope ratios (Fig. 7). This similarity enables annual growth lines to be accurately located on the OSL which coincide with sharp decreases in the Sr/Ca ratio and $\delta^{18}O_{shell}$ values corresponding to colder temperature. In this case, growth cessation of *M. polynyma* could be related to winter temperatures, as already observed for many other high-latitude bivalves (Killam and Clapham, 2018), such as *Arctica islandica* (Weidman et al. 1994), *Hiatella arctica* (Sejr et al., 2002) and *Serripes groenlandicus* (Khim et al., 2003), and cold water temperatures mostly coincide with ice-covered periods. The annual growth lines localization also provides an interesting observation of the inter-annual growth rate variability. Overall, 8 to 10 carbonate samples were micromilled each year except in 2013 (where there were 15 samples; Fig. 3). Since all carbonate samples were equidistant, this suggests a higher growth rate in 2013 than the following years. This could be due to a natural ontogenetic decrease or to environmental changes.

The step-by-step chemochronology methodology allows the location of annual growth lines in a specific portion of the shell that can be matched to a precise calendar year. Once the specimen's age is determined, associated environmental effects can then be explored. Even though the mechanisms causing annual growth line formation for *M. polynyma* are still poorly understood, our results are in agreement with other studies on marine bivalves that have suggested a common control between shell

Sr incorporation and bivalve growth rate (Gillikin et al., 2005; Stecher et al., 1996; Takesue and van Geen, 2004; Vander Putten et al., 2000).

FIGURE 6 (2 columns)

FIGURE 7 (2 columns)

Using the geochemical approach and the date of death (i.e., date of field sampling), we estimated the ages of specimens M07, M08, M10, M14, M15, and M12 to be approximately 11, 12, 21, 21, 21, and 22 years, respectively (Fig. 5). This approach can be applied even if one specimen has an erratic growth pattern compared to the others. For example, despite Ba/Ca ratio variations between specimen M14 and the others are similar (Fig. 4), a delay in two concomitant Sr/Ca ratio drops was noted, indicating punctual slowing in growth for M14 (Fig. 5). This specific anomaly, only observed on M14, was likely caused by a local and probably discrete unknown disturbance, which could reflect a predator attack or any other type of individual disruption.

4.2. Exploration of the growth rates: Regional comparison and intra-site synchrony

In Figure 8, the growth curve of *M. polynyma* from Baie-Comeau was constructed using length-at-age data (i.e., distance from the umbo to each growth line revealed by the chemochronology) (Fig. 8A) that was compared to growth curves calculated either on the external shell (Lambert and Goudreau, 1999; Landry et al., 1992a) or the hinge plate (Bourassa et al., 2008; Roddick et al., 2012; Trottier and Goudreau, 2015) of specimens collected at six other sites. In each case, the von Bertalanffy growth function was used (Fig. 8B; see section 3.4 for details). Shells collected at Baie-Comeau showed a slow growth rate with a maximum size of 146.35 mm (Table 3). Variability in specimen growth rate and longevity can be observed between our sampling (Baie-Comeau) and those from previous studies in the Gulf of St. Lawrence (Table 3; Fig. 8B). Growth estimated with the von Bertalanffy growth

455 function for specimens from the Îles-de-la-Madeleine (L_∞ = 122.37; K = 0.049) was highly different,
456 not only from those in Baie-Comeau (L_∞ = 146.35; K = 0.058) but also from all other sites.
457 Environmental conditions, such as the water depth, the bottom water temperature and salinity as well
458 as the productivity on the sampling site are probably key factors explaining the observed growth
459 differences. Further studies are needed to explore the role of these later parameters on the local
460 growth rates of *M. polynyma* such as multi-annual environmental monitoring.

461

462 FIGURE 8 (2 columns)

463 TABLE 3 (2 columns)

464 Testing the robustness of our growth rate estimation method is difficult because specimens from Baie-
465 Comeau have not previously been the subject of growth studies, so no comparison can be made
466 between the classical sclerochronological method and our geochemical approach. Globally, the
467 growth rate estimated for Baie-Comeau specimens shows a similar trend with North Shore GSL sites
468 and Banquereau Bank, for the first 15 years at least. This corresponds to a specimen length of ~90
469 mm. However, after 15 years, our model predicts a higher growth rate than previously reported. For
470 example, for a length of 130 mm, our model gives an age of 38 years. In Longue-Pointe-de-Mingan
471 (fishing zone 4B, ca. 400 km from Baie-Comeau; Fig. 1b), a length of 130 mm can be reached only
472 for specimens older than 50 years (Bourassa et al., 2008). That length is never reached with the other
473 models, which overestimate the age of *M. polynyma* relative to the model that we calculated. It is
474 currently impossible to separate the environmental factors from the methodological approach to
475 explain these differences, even though Lambert and Goudreau (1999) still noted an overestimation
476 risk due to excess growth lines. Further geochemical investigations on specimens dated in previous
477 studies should be planned to validate the different methodologies. Moreover, a better understanding of
478 growth rate drivers would probably improve bivalve fishery management in the EGSL.

479 FIGURE 9 (1 columns)

480

The chemochronology method provided a reliable method to study growth rate anomalies (SGIs) of *M. polynyma* in Baie-Comeau (Fig. 9). SGIs of the different specimens exhibited chaotic variations before 2010 (with specimen M14; Fig. 9A), highlighted with an EPS value dropping below the threshold of accuracy (e.g., 0.85). By removing the specimen M14, the master chronology showed a higher level of confidence, even if EPS values were still under the arbitrary threshold of 0.85 before 2008 (Fig. 9B). This difference in EPS values before and after 2008 was probably exacerbated by the low number of studied specimens. Indeed, it is rare to obtain a robust master chronology with only three specimens. To date, according to our knowledge, the minimum sample depth leading to a robust master chronology was found to be four shells of *Arctica islandica* (Estrella-Martinez et al., 2019). Nevertheless, both master chronologies obtained in our study showed a strong positive growth anomaly in 2013. This is consistent with the number of $\delta^{18}O_{shell}$ samples—higher than in other years—characterizing 2013 in the OSL of specimen M17. These results underlined a common response among the individuals studied to variations in their environments, demonstrating great potential as environmental archives especially considering the high EPS values after 2008. This technique is promising but more shells are needed to confirm the environmental response.

5. Summary and perspectives

This pioneer work offers an alternative to age bivalve species with misidentified annual growth lines, using shell geochemistry to accurately build an age model. Previous methods using standard sclerochronological techniques may have under- or over-estimated the age of *M. polynyma* shells. Here, we proposed a new methodology based on chemochronology (i.e., using geochemical data) to precisely locate annual growth lines (Fig. 2). The present study showed (i) the utility of the $\delta^{18}O$ profile to reveal disturbance lines among non-identified annual growth lines in the outer shell layer, and (ii) the strong relationship between Ba/Ca and Sr/Ca ratios that allowed the alignment and localization, respectively, of annual growth lines with a high level of confidence. The presence of

common sharp Sr/Ca ratio decreases between aligned profiles provided information on the position of single annual growth lines.

This chemochronological approach made it possible to reconstruct the temporal variations of standardized growth indices (i.e., master chronology) between 1998 and 2017. Our results highlighted that SGI variations are highly synchronous between specimens after 2008. Therefore, *M. polynyma* shells likely have a great potential for reconstructing past environment conditions before the instrumental era if enough specimens are available and fulfil specific criteria (i.e., over a size spectrum and state of preservation). Furthermore, synchronous trace element profiles between contemporaneous specimens could inform on past environmental variability. Indeed, numerous study linked peaks of Ba/Ca ratios to phytoplankton dynamics (e.g., Doré et al., 2020; Stecher et al., 1996; Thébault et al., 2009; Vander Putten et al., 2000). Further investigation should be done to compare variations of SGI and trace element time series with local and regional environmental variability (e.g., fluctuations in water temperature, primary production) in order to calibrate these tools as environmental proxies. All these findings support the idea that *M. polynyma* is a promising biogenic archive that could be integrated into future environmental studies of the coastal zone in sub-arctic ecosystems.

Acknowledgements:

This research is a contribution of LIA-BeBest, an international collaboration between French (IUEM-UBO, LEMAR - Brest) and Canadian (ISMER-UQAR, Rimouski) academic institutions. We thank LEMAR and DFO personnel for their help. We are sincerely grateful to crew and science staff onboard the CCGS *Leim* for their dedicated help during sampling. In addition, we express our sincere gratitude to staff at the Research Centre on the Dynamics of the Earth System (GEOTOP), particularly to André Poirier for his useful help and efficiency. We would also like to thank the employees of Pôle Spectrométrie Océan (PSO, Plouzané, France) for their hard work in adjusting the analysis method at our request. We show our appreciation to Laure Devine for her useful comments. This research was supported by a grant from the Natural Sciences and Engineering Research Council

of Canada (to G.C.) and the Canada Research Chair Program (to G.C.) as well as the University of Occidental Brittany and LabeX Mer. All data used to produce the results of this paper may be obtained by contacting the corresponding author.

Sample CRediT author statement

Justine Doré: Methodology, Writing- Original draft preparation, Conceptualization, Visualization

Julien Thébault, Gwénaëlle Chaillou, Virginie Roy, Fabien Dewilde: Conceptualization

Fabien Dewilde: Methodology

Julien Thébault, Gwénaëlle Chaillou, Virginie Roy, Fabien Dewilde: Writing- Review & Editing

Supplementary figures:

Fig. 1S. Diagram of the step-by-step approach used to identify annual growth lines on hinge plates and to determine growth rate of *Mactromeris polynyma* specimens

Fig. 2S. Locations of salinity and $\delta^{18}O_{sw}$ measurements made by Tan and Strain between 1980 and 1996 that were used to calculate the linear regression used in eq. (2).

Fig. 3S. Photographs of the hinge plate of specimen M07 using different optic tools and treatments. (A) Shell was polished and then photographed with a stereo-microscope at 20x magnification. (B) Shell after treatment with Mutvei's solution and photographed with a digital microscope at 500x magnification. (C) Mosaic of images (500x magnification) showing the whole hinge plate.

References

Abele, D., Brey, T., Philipp, E., 2009. Bivalve models of aging and the determination of molluscan lifespans. Exp. Gerontol. 44, 307–315. https://doi.org/10.1016/j.exger.2009.02.012

Ballesta-Artero, I., Zhao, L., Milano, S., Mertz-Kraus, R., Schöne, B.R., van der Meer, J., Witbaard, R., 2018. Environmental and biological factors influencing trace elemental and microstructural properties of *Arctica islandica* shells. Sci. Total Environ. 645, 913–923. https://doi.org/10.1016/j.scitotenv.2018.07.116

Black, H.D., Andrus, C.F.T., Lambert, W.J., Rick, T.C., Gillikin, D.P., 2017. $\delta^{15}N$ values in *Crassostrea virginica* shells provides early direct evidence for nitrogen loading to Chesapeake Bay. Sci. Rep. 7, 44241. https://doi.org/10.1038/srep44241

Blais, M., Galbraith, P.S., Plourde, S., Scarratt, M., Devine, L., Lehoux, C., 2019. Chemical and biological oceanographic conditions in the Estuary and Gulf of St. Lawrence during 2018. Can. Sci. Advis. Sec. Res. Doc. 2019/059, iv + 64 pp.

Bourassa, L., Giguère, M., Brulotte, C., Cyr, C., Perreault, L., 2008. Evaluation de la croissance, du taux d'exploitation et du recrutement à la pêche de la mactre de Stimpson (*Mactromeris polynyma*) de la Moyenne-Côte-Nord, Québec. Rapp. tech. can. sci. halieut. aquat. 2799 x + 39 p.

Bourdages, H., Goudreau, P., Lambert, J., Landry, L., Nozères, C., 2012. Distribution des bivalves et gastéropodes benthiques dans les zones infralittorale et circalittorale des côtes de l'estuaire et du nord du golfe du Saint-Laurent. Rapp. tech. can. sci. halieut. aquat. 3004: iv + 103 p.

Brulotte, S., 1995. Distribution et abondance relative de la mactre de Stimpson en Haute-Côte Nord et en Gaspésie. Programme d'adaptation des pêches de l'Atlantique (Canada). No 57, 25 p.

Bunn, A.G., 2008. A dendrochronology program library in R (dplR). Dendrochronologia 26, 115–124. https://doi.org/10.1016/j.dendro.2008.01.002

Butler, P.G., Richardson, C.A., Scourse, J.D., Wanamaker, A.D., Shammon, T.M., Bennell, J.D., 2010. Marine climate in the Irish Sea: analysis of a 489-year marine master chronology derived from growth increments in the shell of the clam *Arctica islandica*. Quat. Sci. Rev. 29, 1614–1632. https://doi.org/10.1016/j.quascirev.2009.07.010

Cardoso, J.F., Santos, S., Witte, J.I., Witbaard, R., van der Veer, H.W., Machado, J.P., 2013a. Validation of the seasonality in growth lines in the shell of *Macoma balthica* using stable isotopes and trace elements. J. Sea Res. 82, 93–102. https://doi.org/10.1016/j.seares.2012.09.006

Cardoso, J.F., Nieuwland, G., Witbaard, R., van der Veer, H.W., Machado, J.P., 2013b. Growth increment periodicity in the shell of the razor clam *Ensis directus* using stable isotopes as a method to validate age. Biogeosciences 10, 4741–4750. https://doi.org/10.5194/bg-10-4741-2013

Carré, M., Bentaleb, I., Bruguier, O., Ordinola, E., Barrett, N.T., Fontugne, M., 2006. Calcification rate influence on trace element concentrations in aragonitic bivalve shells: Evidences and mechanisms. Geochim. Cosmochim. Acta 70, 4906–4920. https://doi.org/10.1016/j.gca.2006.07.019

Coplen, T.B., 1996. Editorial: More uncertainty than necessary. Paleoceanogr. Curr. 11, 369–370.

Cyr, C., 1994. Pêche exploratoire de la mactre de Stimpson en Moyenne et Basse Côte-Nord du Québec. Programme d'adaptation des pêches de l'Atlantique (Canada). No 54, 21

Degtlareva, A., Elektorowicz, M., 2001. A computer simulation of water quality change due to dredging of heavy metals contaminated sediments in the Old Harbour of Montreal. Water Qual. Res. J. Canada 36, 1–19. https://doi.org/10.2166/wqrj.2001.001

Devine, L., Scarratt, M., Plourde, S., Galbraith, P.S., Michaud, S., and Lehoux, C. 2017. Chemical and Biological Oceanographic Conditions in the Estuary and Gulf of St. Lawrence during 2015. DFO Can. Sci. Advis. Sec. Res. Doc. 2017/034. v + 48 pp.

DFO, 2018. Assessment of the Stimpson's surfclam stocks of Quebec coastal water in 2017. DFO Can. Sci. Advis. Sec. Sci. Advis. Rep. 2018/022.

DFO, 2006. Impacts of trawl gears and scallop dredges on benthic habitats, populations and communities. DFO Can. Sci. Advis. Sec. Sci. Advis. Rep. 2006/025

Dodd, J.R., 1965. Environmental control of strontium and magnesium in *Mytilus*. Geochim. Cosmochim. Acta 29, 385–398.

Dodd, J.R., Crisp, E.L., 1982. Non-linear variation with salinity of Sr/Ca and Mg/Ca ratios in water and aragonitic bivalve shells and implications for paleosalinity studies. Palaeogeogr. Palaeoclimatol. Palaeoecol. 38, 45–56. https://doi.org/10.1016/0031-0182(82)90063-3

Doré, J., Chaillou, G., Poitevin, P., Lazure, P., Poirier, A., Chauvaud, L., Archambault, P., Thébault, J., 2020. Assessment of Ba/Ca in *Arctica islandica* shells as a proxy for phytoplankton dynamics in the Northwestern Atlantic Ocean. Estuar. Coast. Shelf Sci. 237, 106628. https://doi.org/10.1016/j.ecss.2020.106628

Druffel, E.R.M., 1997. Geochemistry of corals: Proxies of past ocean chemistry, ocean circulation, and climate. Proc. Natl. Acad. Sci. 94, 8354–8361. https://doi.org/10.1073/pnas.94.16.8354

Dufour, R., Ouellet, P., 2007. Estuary and Gulf of St. Lawrence marine ecosystem overview and assessment Report. Can. Tech. Rep. Fish. Aquat. Sci. 2744E: vii + 112p.

Dutil, J., Proulx, S., Galbraith, P.S., Chassé, J., Lambert, N., Laurian, C., 2012. Coastal and epipelagic habitats of the estuary and Gulf of St . Lawrence. Can. Tech. Rep. Fish. Aquat. Sci. 3009 ix + 87 pp.

Dunca, E., Schöne, B.R., Mutvei, H., 2005. Freshwater bivalves tell of past climates: But how clearly do shells from polluted rivers speak? Palaeogeogr. Palaeoclimatol. Palaeoecol. 228, 43–57. https://doi.org/10.1016/j.palaeo.2005.03.050

Estrella-Martínez, J., Ascough, P.L., Schöne, B.R., Scourse, J.D., Butler, P.G., 2019. 8.2 ka event North Sea hydrography determined by bivalve shell stable isotope geochemistry. Sci. Rep. 9, 6753. https://doi.org/10.1038/s41598-019-43219-1

Fenger, T., Surge, D., Schöne, B., Milner, N., 2007. Sclerochronology and geochemical variation in limpet shells (*Patella vulgata*): a new archive to reconstruct coastal sea surface temperature. Geochemistry, Geophys. Geosystems 8. https://doi.org/10.1029/2006GC001488

Foster, L.C., Allison, N., Finch, A.A., Andersson, C., 2009. Strontium distribution in the shell of the aragonite bivalve *Arctica islandica*. Geochemistry, Geophys. Geosystems 10. https://doi.org/10.1029/2007GC001915

Freitas, P.S., Clarke, L.J., Kennedy, H., Richardson, C.A., Abrantes, F., 2006. Environmental and biological controls on elemental (Mg/Ca, Sr/Ca and Mn/Ca) ratios in shells of the king scallop *Pecten maximus*. Geochim. Cosmochim. Acta 70, 5119–5133. https://doi.org/10.1016/j.gca.2006.07.029

Galbraith, P.S., Chassé, J., Caverhill, C., Nicot, P., Gilbert, D., Lefaivre, D., Lafleur, C., 2019. Physical oceanographic conditions in the Gulf of St. Lawrence during 2018. DFO Can. Sci. Advis. Sec. Res. Doc. 2019/046. v + 79 p.

Genovesi, L., de Vernal, A., Thibodeau, B., Hillaire-Marcel, C., Mucci, A., Gilbert, D., 2011. Recent changes in bottom water oxygenation and temperature in the Gulf of St. Lawrence: Micropaleontological and geochemical evidence. Limnol. Oceanogr. 56, 1319–1329. https://doi.org/10.4319/lo.2011.56.4.1319

Gilbert, D., Chabot, D., Archambault, P., Hébert, S., 2007. Appauvrissement en oxygène dans les eaux profondes du Saint-Laurent marin. Le Nat. Can. 131, 67–75.

Gilbert, D., Sundby, B., Gobeil, C., Mucci, A., Tremblay, G.-H., 2005. A seventy-two-year record of diminishing deep-water oxygen in the St. Lawrence estuary: The northwest Atlantic connection. Limnology and Oceanography 50, 1654–1666. https://doi.org/10.4319/lo.2005.50.5.1654

Gilbert, M., Dufour, R., 2008. The Gulf of St. Lawrence marine ecosystem: An overview of its structure and dynamics, human pressures, and governance approaches. 2008/J:18.

Gillikin, D.P., Dehairs, F., Lorrain, A., Steenmans, D., Baeyens, W., André, L., 2006. Barium uptake into the shells of the common mussel (*Mytilus edulis*) and the potential for estuarine paleo-chemistry reconstruction. Geochim. Cosmochim. Acta 70, 395–407. https://doi.org/10.1016/j.gca.2005.09.015

Gillikin, D.P., Lorrain, A., Navez, J., Taylor, J.W., André, L., Keppens, E., Baeyens, W., Dehairs, F., 2005. Strong biological controls on Sr/Ca ratios in aragonitic marine bivalve shells. Geochemistry, Geophys. Geosystems 6.

Griffin, S.M., 2012. Applying dendrochronology visual crossdating techniques to the marine bivalve *Arctica islandica* and assessing the utility of master growth chronologies as proxies for temperature and secondary productivity in the Gulf of Maine. Doctoral dissertation, Iowa State University, Ames, IA, 237 pp.

Grossman, E.L., Ku, T.-L., 1986. Oxygen and carbon isotope fractionation in biogenic aragonite: Temperature effects. Chem. Geol. Isot. Geosci. Sect. 59, 59–74. https://doi.org/10.1016/0168-9622(86)90057-6

Gurney, L.J., Mundy, C., Porteus, M.C., 2005. Determining age and growth of abalone using stable oxygen isotopes: a tool for fisheries management. Fish. Res. 72, 353–360. https://doi.org/10.1016/j.fishres.2004.12.001

Hudson, J.H., Shinn, E.A., Halley, R.B., Lidz, B., 1976. Sclerochronology: a tool for interpreting past environments. Geology 4, 361–364.

Hut, G., 1987. Consultants' group meeting on stable isotope reference samples for geochemical and hydrological investigations.

Jones, D.S., 1983. Sclerochronology: reading the record of the molluscan shell: annual growth increments in the shells of bivalve molluscs record marine climatic changes and reveal surprising longevity. Am. Sci. 71, 384–391.

Jutras, M., Mucci, A., Sundby, B., Gratton, Y., Katsev, S., 2020. Nutrient cycling in the Lower St. Lawrence Estuary: Response to environmental perturbations. Estuar. Coast. Shelf Sci. 239, 106715. https://doi.org/10.1016/j.ecss.2020.106715

Khim, B.-K., Krantz, D.E., Cooper, L.W., Grebmeier, J.M., 2003. Seasonal discharge of estuarine freshwater to the western Chukchi Sea shelf identified in stable isotope profiles of mollusk shells. J. Geophys. Res. 108, 3300. https://doi.org/10.1029/2003JC001816

Kilada, R.W., Campana, S.E., Roddick, D., 2009. Growth and sexual maturity of the northern propeller clam (*Cyrtodaria siliqua*) in Eastern Canada, with bomb radiocarbon age validation. Mar. Biol. 156, 1029–1037. https://doi.org/10.1007/s00227-009-1146-9

Kilada, R.W., Campana, S.E., Roddick, D., 2007. Validated age, growth, and mortality estimates of the ocean quahog (*Arctica islandica*) in the western Atlantic. ICES J. Mar. Sci. 64, 31–38. https://doi.org/10.1093/icesjms/fsl001

Killam, D., Clapham, M., 2018. Identifying the ticks of bivalve shell clocks: seasonal growth in relation to temperature and food supply. Palaios 33, 228–236. https://doi.org/10.2110/palo.2017.072

Klein, R.T., Lohmann, K.C., Thayer, C.W., 1996. SrCa and $^{13}C^{12}C$ ratios in skeletal calcite of *Mytilus trossulus*: Covariation with metabolic rate, salinity, and carbon isotopic composition of seawater. Geochim. Cosmochim. Acta 60, 4207–4221. https://doi.org/10.1016/S0016-7037(96)00232-3

Klein, R., & Witbaard, R. (1993). The appearance of scars on the shell of *Arctica islandica L.*(Mollusca, Bivalvia) and their relation to bottom trawl fishery. *NIOZ-rapport*, *12*.

Lambert, J., Giguère, M., 1994. Développement de la pêche à la mactre de Stimpson (*Mactromeris polynyma*) au Québec et efficacité de la drague hydraulique de type Nouvelle-Angleterre. In The development of underutilized invertebrate fisheries in eastern Canada. Edited by L. Gendron and S. Robinson. Can. Manus. Rep. Fish. Aquat. Sci. 2247, 73-81.

Lambert, J., Goudreau, P., 1995a. Mactre de Stimpson et couteau des côtes du Québec. *In* Savard, L. (ed) 1995. Rapport sur l'état des invertébrés en 1994 : crustacés et mollusques des côtes du Québec, crevette nordique et zooplancton de l'estuaire et du golfe du Saint-Laurent. Rapp. manus. can. sci. halieut. aquat. 2323, 137 p.

Lambert, J., Goudreau, P., 1995b. Performance de la drague hydraulique de type Nouvelle-Angleterre pour la récolte de la mactre de Stimpson (*Mactromeris polynyma*). Rapp. tech. can. sci. halieut. aquat. 235, 28.

Lambert, J., Goudreau, P., 1997. Biologie et exploitation de la mactre de Stimpson, *Mactromeris polynyma*, sur les côtes du Québec. MPO, Sec. can. éval. stock, Doc. Rech. 97/101. 44.

Lambert, J., Goudreau, P., 1999. Indices de croissance de la mactre de Stimpson (*Mactromeris polynyma*). Rapp. tech. can. sci. halieut. aquat. 2269 : vii + 39 p

Landry, T., Wade, E., Giguère, M., 1992. Évaluation de gisements de Mactre de Stimpson, *Mactromeris polynyma*, dans le golfe du Saint-Laurent : résultats préliminaires. Secr. Can. Consult. Sci. Du MPO, Doc. Rech. 92, 86.

Langlet, D., Renard, M., Roux, M., Schein, E., 2002. Biological versus environmental control on shell chemistry of the vent clam *Calyptogena magnifica*. Cah. Biol. Mar. 43, 253–258.

Lavoie, D., Starr, M., Zakardjian, B., Larouche, P., 2007 Identification of ecologically and biologically significant areas (EBSA) in the Estuary and Gulf of St. Lawrence: Primary production. CSAS Res. Doc. 2007/079, 33.

DFO, 2007. Ecologically and Biologically Significant Areas (EBSA) in the Estuary and Gulf of St. Lawrence: identification and characterization. DFO Can. Sci. Advis. Sec., Sci. Adv. Rep. 2007/016.

Lazareth, C., Putten, E.V., André, L., Dehairs, F., 2003. High-resolution trace element profiles in shells of the mangrove bivalve *Isognomon ephippium*: a record of environmental spatio-temporal variations? Estuar. Coast. Shelf Sci. 57, 1103–1114. https://doi.org/10.1016/S0272-7714(03)00013-1

Lea, D.W., Shen, G.T., Boyle, E.A., 1989. Coralline barium records temporal variability in equatorial Pacific upwelling. Nature 340, 373–376.

Lefort, S., Mucci, A., Sundby, B., 2012. Sediment response to 25 years of persistent hypoxia. Aquat. Geochemistry 18, 461–474. https://doi.org/10.1007/s10498-012-9173-4

Lorrain, A., Gillikin, D.P., Paulet, Y.-M., Chauvaud, L., Mercier, A. Le, Navez, J., André, L., 2005. Strong kinetic effects on Sr/Ca ratios in the calcitic bivalve *Pecten maximus*. Geology 33, 965. https://doi.org/10.1130/G22048.1

Mann, R., Munroe, D.M., Powell, E.N., Hofmann, E.E., Klinck, J.M., 2013. Bivalve molluscs: Barometers of climate change in arctic marine systems, in Mueter, F.J., Dickson, D.M.S., Huntington, H.P., Irvine J.R., Logerwell, E.A., MacLean, S.A., Quakenbush, L.T., Rosa, C. (Eds.), Responses of arctic marine

ecosystems to climate change. Alaska Sea Grant Program, on-line publication. https://doi.org/10.4027/ramecc.2013.04

Marali, S., Schöne, B.R., Mertz-Kraus, R., Griffin, S.M., Wanamaker, A.D., Matras, U., Butler, P.G., 2017. Ba/Ca ratios in shells of *Arctica islandica* – Potential environmental proxy and crossdating tool. Palaeogeogr. Palaeoclimatol. Palaeoecol. 465, 347–361. https://doi.org/10.1016/j.palaeo.2015.12.018

Mucci, A., Starr, M., Gilbert, D., Sundby, B., 2011. Acidification of Lower St. Lawrence estuary bottom waters. Atmos. - Ocean 49, 206–218. https://doi.org/10.1080/07055900.2011.599265

Pearce, N.J.G., Mann, V.L., 2006. Trace metal variations in the shells of *Ensis siliqua* record pollution and environmental conditions in the sea to the west of mainland Britain. Mar. Pollut. Bull. 52, 739–755. https://doi.org/10.1016/j.marpolbul.2005.11.003

Poulain, C., Gillikin, D.P., Thébault, J., Munaron, J.M., Bohn, M., Robert, R., Paulet, Y.-M., Lorrain, A., 2015. An evaluation of Mg/Ca, Sr/Ca, and Ba/Ca ratios as environmental proxies in aragonite bivalve shells. Chem. Geol. 396, 42–50. https://doi.org/10.1016/j.chemgeo.2014.12.019

Prendergast, A.L., Versteegh, E.A.A., Schöne, B.R., 2017. New research on the development of high-resolution palaeoenvironmental proxies from geochemical properties of biogenic carbonates. Palaeogeogr. Palaeoclimatol. Palaeoecol. 484, 1–6. https://doi.org/10.1016/j.palaeo.2017.05.032

Ramsay, K., Kaiser, M.J., Richardson, C.A., Veale, L.O., Brand, A.R., 2000. Can shell scars on dog cockles (*Glycymeris glycymeris L.*) be used as an indicator of fishing disturbance? J. Sea Res. 43, 167–176. https://doi.org/10.1016/S1385-1101(00)00006-X

Rhoads, D.C., Lutz, R.A., 1980. Growth patterns within the molluscan shell: an overview, in: Rhoads, D.C., Lutz, R.A. (Eds.), Skeletal growth of aquatic organisms. Biological records of environmental change, topics in geobiology. Plenum Press, New York, pp. 203–254.

Richardson, C.A., 2001. Molluscs as archives of environmental change. Ocean. Mar. Biol. 39, 103–164.

Richardson, C.A., Peharda, M., Kennedy, H., Kennedy, P., Onofri, V., 2004. Age, growth rate and season of recruitment of *Pinna nobilis* (L) in the Croatian Adriatic determined from Mg:Ca and Sr:Ca shell profiles. J. Exp. Mar. Bio. Ecol. 299, 1–16. https://doi.org/10.1016/j.jembe.2003.08.012

Robinson, R. F., & Richardson, C. A. (1998). The direct and indirect effects of suction dredging on a razor clam (Ensis arcuatus) population. *ICES Journal of Marine Science*, *55*(5), 970-977.

Roddick, D., Brading, L., Carrigan, L., Davignon-Burton, T., Graham, S., McEwen, C., 2012. Assessment of the Arctic Surfclam (*Mactromeris polynyma*) stock on Banquereau in 2010. DFO Can. Sci. Advis. Sec. Res. Doc. 2012/050. iii + 60 p.

Rosenberg, G.D., Runcorn, S.K., 1975. Growth rhythms and the history of the earth's rotation; Proceedings of the Interdisciplinary Winter Conference on Biological Clocks and Changes in the Earth's Rotation: Geophysical and Astronomical Consequences, University of Newcastle-upon-Tyne, Newcastle-upon-Tyne, England, January 8-10, 1974

Savenkoff, C., Bourassa, M.-N., Baril, D., Benoît, H.P., 2007. Identification of Ecologically and Biologically Significant Areas for the Estuary and Gulf of St. Lawrence, 2007/015.

Schöne, B.R., 2008. The curse of physiology - Challenges and opportunities in the interpretation of geochemical data from mollusk shells. Geo-Marine Lett. 28, 269–285. https://doi.org/10.1007/s00367-008-0114-6

Schöne, B.R., 2013. *Arctica islandica* (Bivalvia): A unique paleoenvironmental archive of the northern North Atlantic Ocean. Glob. Planet. Change 111, 199–225. https://doi.org/10.1016/j.gloplacha.2013.09.013

Schöne, B.R., Dunca, E., Fiebig, J., Pfeiffer, M., 2005. Mutvei's solution: An ideal agent for resolving microgrowth structures of biogenic carbonates. Palaeogeogr. Palaeoclimatol. Palaeoecol. 228, 149–166. https://doi.org/10.1016/j.palaeo.2005.03.054

Schöne, B.R., Radermacher, P., Zhang, Z., Jacob, D.E., 2013. Crystal fabrics and element impurities (Sr/Ca, Mg/Ca, and Ba/Ca) in shells of *Arctica islandica*—Implications for paleoclimate reconstructions. Palaeogeogr. Palaeoclimatol. Palaeoecol. 373, 50–59. https://doi.org/10.1016/j.palaeo.2011.05.013

Schöne, B.R., Surge, D.M., 2012. Part N, Revised, Volume 1, Chapter 14: Bivalve sclerochronology and geochemistry. Treatise Online 46, 1–24.

Scourse, J., Richardson, C., Forsythe, G., Harris, I., Heinemeier, J., Fraser, N., Briffa, K., Jones, P., 2006. First cross-matched floating chronology from the marine fossil record: Data from growth lines of the long-lived bivalve mollusc *Arctica islandica*. Holocene 16, 967–974. https://doi.org/10.1177/0959683606hl987rp

Sejr, M.K., Jensen, T.K., Rysgaard, S., 2002. Annual growth bands in the bivalve *Hiatella arctica* validated by a mark-recapture study in NE Greenland. Polar Biol. 25, 794–796. https://doi.org/10.1007/s00300-002-0413-8

Stecher, H.A., Krantz, D.E., Lord, C.J., Luther, G.W., Bock, K.W., 1996. Profiles of strontium and barium in *Mercenaria mercenaria* and *Spisula solidissima* shells. Geochim. Cosmochim. Acta 60, 3445–3456. https://doi.org/10.1016/0016-7037(96)00179-2

Strom, A., Francis, R.C., Mantua, N.J., Miles, E.L., Peterson, D.L., 2004. North Pacific climate recorded in growth rings of geoduck clams: a new tool for paleoenvironmental reconstruction. Geophys. Res. Lett. 31. https://doi.org/10.1029/2004GL019440

Takesue, R.K., van Geen, A., 2004. Mg/Ca, Sr/Ca, and stable isotopes in modern and Holocene *Protothaca staminea* shells from a northern California coastal upwelling region. Geochim. Cosmochim. Acta 68, 3845–3861.

Thébault, J., Chauvaud, L., L'Helguen, S., Clavier, J., Barats, A., Jacquet, S., Pécheyran, C., Amouroux, D., 2009. Barium and molybdenum records in bivalve shells: geochemical proxies for phytoplankton dynamics in coastal environments. Limnol. Oceanogr. 54, 1002–1014. https://doi.org/10.4319/lo.2009.54.3.1002

Thibodeau, B., de Vernal, A., Mucci, A., 2006. Recent eutrophication and consequent hypoxia in the bottom waters of the Lower St. Lawrence Estuary: Micropaleontological and geochemical evidence. Mar. Geol. 231, 37–50. https://doi.org/10.1016/j.margeo.2006.05.010

Thompson, I., Jones, D.S., Dreibelbis, D., 1980. Annual internal growth banding and life history of the ocean quahog *Arctica islandica* (Mollusca: Bivalvia). Mar. Biol. 57, 25–34.

Trottier, S., Goudreau, P., 2015. Evaluation des stocks de mactre de Stimpson (*Mactromeris polynyma*) des eaux côtières du Québec en 2014. Secr. can. Consult. sci. du MPO. Doc. rech. 2015/063. ix + 72 p.

Vander Putten, E., Dehairs, F., Keppens, E., Baeyens, W., 2000. High resolution distribution of trace elements in the calcite shell layer of modern *Mytilus edulis*: Environmental and biological controls. Geochim. Cosmochim. Acta 64, 997–1011. https://doi.org/10.1016/S0016-7037(99)00380-4

Walliser, E.O., Schöne, B.R., Tütken, T., Zirkel, J., Grimm, K.I., Pross, J., 2015. The bivalve *Glycymeris planicostalis* as a high-resolution paleoclimate archive for the Rupelian (Early Oligocene) of central Europe. Clim. Past 11, 653–668. https://doi.org/10.5194/cp-11-653-2015

Wanamaker, A.D., Baker, A., Butler, P.G., Richardson, C.A., Scourse, J.D., Ridgway, I., Reynolds, D.J., 2009. A novel method for imaging internal growth patterns in marine mollusks: A fluorescence case study on the aragonitic shell of the marine bivalve *Arctica islandica* (Linnaeus). Limnol. Oceanogr. Methods 7, 673–681. https://doi.org/10.4319/lom.2009.7.673

Wanamaker, A.D., Gillikin, D.P., 2019. Strontium, magnesium, and barium incorporation in aragonitic shells of juvenile *Arctica islandica*: Insights from temperature controlled experiments. Chem. Geol. 526, 117–129. https://doi.org/10.1016/j.chemgeo.2018.02.012

Wanamaker, A.D., Heinemeier, J., Scourse, J.D., Richardson, C.A., Butler, P.G., Eiríksson, J., Knudsen, K.L., 2008. Very long-lived mollusks confirm 17th century ad tephra-based radiocarbon reservoir ages for north icelandic shelf waters. Radiocarbon 50, 399–412. https://doi.org/https://doi.org/10.1017/S0033822200053510

Weidman, C.R., Jones, G.A., 1994. The long-lived mollusc *Arctica islandica*: A new paleoceanographic tool for the reconstruction of bottom temperatures for the continental shelves of the northern North Atlantic Ocean. J. Geophys. Res. 99, 18305. https://doi.org/10.1029/94JC01882

Wigley, T.M.L., Briffa, K.R., Jones, P.D., 1984. On the average value of correlated time series, with applications in dendroclimatology and hydrometeorology. J. Clim. Appl. Meteorol. 23, 201–213. https://doi.org/10.1175/1520-0450(1984)023<0201:OTAVOC>2.0.CO;2

Witbaard, R., 1997. Tree of the sea: The use of the internal growth lines in the shell of *Arctica islandica* (Bivalvia, Mollusca) for the retrospective assessment of marine environmental change.

Witbaard, R., Jenness, M.I., Van Der Borg, K., Ganssen, G., 1994. Verification of annual growth increments in *Arctica islandica* L. from the North Sea by means of oxygen and carbon isotopes. Netherlands J. Sea Res. 33, 91–101. https://doi.org/10.1016/0077-7579(94)90054-X

Witbaard, R., & Klein, R. (1994). Long-term trends on the effects of the southern North Sea beamtrawl fishery on the bivalve mollusc *Arctica islandica* L.(Mollusca, bivalvia). *ICES Journal of Marine Science*, *51*(1), 99-105.

Figure captions

Fig. 1. Map of DFO fishing areas for *Mactromeris polynyma* in the Estuary and Gulf of St. Lawrence. (A) Location of the Estuary and Gulf of St. Lawrence, (B) DFO fishing areas with specific beds, and (C) beds of *M. polynyma* with the location of the sample site (purple triangle).

Fig. 2. (A) Schematic of the different cut axes made on *M. polynyma* shells to obtain cross sections used for geochemical analyses. Red dashed lines indicate the maximum growth axis on which geochemical analyses were performed. (B) Image of the hinge plate cross section where trace element analyses (TEA) were performed using LA-ICP-MS. (C) Image of the whole shell cross section (from the umbo to the ventral margin). Two kinds of geochemical analyses were performed: (D) trace element analyses (TEA) and (E) oxygen stable isotope analyses (SIA) in the outer shell layer. Note that SIA was only performed on specimen M17.

Fig. 3. Temporal variations in the theoretical monthly $\delta^{18}O$ (red line) on a 22.4 mm section calculated with eq. (2) and $\delta^{18}O$ measured in the OSL of the specimen M17 (black line). Each coloured dot represents the theoretical value of $\delta^{18}O_{theo}$ calculated using average monthly temperatures and salinities measured between 2010 and 2018. The grey area represents the $\delta^{18}O_{theo}$ standard deviation. The vertical dashed grey lines show the location of growth lines visually identified on the OSL. The dashed black lines are presumed annual growth lines based on $\delta^{18}O_{shell}$ (see section 4.1.2). Note that the y-axis is reversed. DOG: Direction of growth.

Fig. 4. Ba/Ca profiles measured in HPs of six specimens (M15, M07, M08, M10, M12, and M14) from the end of the HP toward the umbo. Grey lines represent the raw data and coloured lines the 10-point running mean. Triangles mark the peaks used to align the profiles. DOG: Direction of growth.

Fig. 5. Aligned profiles of Sr/Ca based on Ba/Ca peaks for the six studied specimens (HPs analyzed). Dashed vertical lines indicate drastic Sr/Ca decreases detectable in all specimens. Triangles mark minimum values of Sr/Ca near or at the dotted lines. DOG: Direction of growth.

Fig. 6. Profile of the Sr/Ca ratio of specimen M10 and photograph of its hinge plate. Vertical dashed grey lines represent minimum Sr/Ca ratio values that are common among specimen profiles; their respective distances from the end of the ventral margin are displayed on the hinge plate photograph (blue arrows). The dashed blue lines show the growth lines associated with arrows.

Fig. 7. Variations in the $\delta^{18}O_{shell}$ and trace element ratios measured from the ventral margin toward the umbo in the OSL are shown. Profiles were smoothed with a 100-point running mean. The red curve presents the Ba/Ca profiles recorded on the M17 OSL and the grey curves show Ba/Ca profiles recorded on the HPs of the 6 other specimens (M07, M08, M12, M10, M15 and M14). Triangles show the average position of annual growth lines among the 6 HPs (see Figure 5); vertical dashed grey lines represent the excessive number of growth lines visually identifiable on the OSL while vertical dashed black lines represent the location of annual growth lines determined by both coupled Ba/Ca and Sr/Ca ratios and oxygen stable isotope ratio ($\delta^{18}O$). Note that the y-axis of $\delta^{18}O_{shell}$ is reversed. DOG: Direction of growth.

Fig. 8. (A) Von Bertalanffy growth curves estimated from the length-at-age of the six studied specimens (i.e., six analyzed HPs) from age 1 to 22 collected in Baie-Comeau. Shell M17 was not added to the curve because its age was unknown. (B) Growth curves calculated to age 70 and estimated for specimens originated from five different beds studied previously in the Gulf of St. Lawrence.

Fig. 9. Standardized annual growth rates (SGIs) of *M. polynyma* shells determined by localization annual growth lines *via* comparisons of inter-individual Sr/Ca ratio patterns. Coloured dots and lines represent the SGIs for the six specimens (A) and without specimen M14 (B) with the averaged chronologies (black). The number of shells in the chronology through time (sample depth) is represented by the grey shadow. EPS values (green curve) from the master chronologies were computed with a five-year running window with an overlap of three years.

Tables

Table 1. Morphometry of collected specimens. The length (anterior–posterior axis), height (dorso–ventral axis) and hinge length for the seven shells are in mm. HP: hinge plate (first 6 shells); OSL: outer shell layer.

	Shell ID	Length	Height	Hinge length
HP	M07	77.48	57.47	9.26
	M08	87.75	65.97	10.77
	M10	104.06	78.94	13.28
	M12	103.55	78.08	13.29
	M14	99.25	73.5	12
	M15	109.14	83.06	14.14
OSL	M17	86.28	65.47	10.66

Table 2. Pairwise correlation matrix between the six hinge plate profiles (M07, M08, M10, M12, M14, and M15) of Sr/Ca (10-pt running mean). Coefficients of correlation (r) were calculated after Sr/Ca profiles were aligned using Ba/Ca peaks (see Fig. 7). Stars indicate the *p*-value: *** <0.001, ** <0.01, * <0.05.

		M07	M08	M10	M12	M14	M15
Sr/Ca	**M07**						
	M08	0.52 ***					
	M10	0.30 ***	0.39 ***				
	M12	0.39 ***	0.28 ***	0.57 ***			
	M14	0.12 ***	0.28 ***	0.49 ***	0.42 ***		
	M15	0.08 *	0.29 ***	0.61 ***	0.61 ***	0.31 ***	

Table 3. Parameters estimated from the von Bertalanffy growth function for six different beds located in the Gulf of St. Lawrence (see Fig. 1B for details). The length reached after an infinite time of growth (L_∞), the Brody growth constant per year (K), and the theoretical age at which the length would be zero, in years (t_0). The associated standard deviation (sd) and 95% confidence interval (CI) is shown only for the Baie-Comeau bed. Sampling years and references for other studies are also given.

Beds	Year	L_∞	K	t_0	References
Baie-Comeau	2018	142.46 *sd = 10.29* *CI ± 20.41*	0.06464 *sd = 0.0082* *CI ± 0.01634*	0.9126 *sd = 0.2103* *CI ± 0.4169*	This study
Longue-Pointe-de-Mingan	2004	134.00	0.0686	0.2120	Bourassa et al., 2008
Moisie River	1993	119.47	0.0825	0.1926	Lambert and Goudreau, 1999
Rivière-au-Tonnerre	1994	110.63	0.0980	0.4870	Lambert and Goudreau, 1999
Iles de la Madelaine	1992	122.37	0.0490	-0.8990	Landry et al., 1992
Banquereau Bank	2010	119.56	0.0830	0.0980	Roddick et al., 2012
Natashquan	2010	125.52	0.0777	0.5899	Trottier and Goudreau, 2015

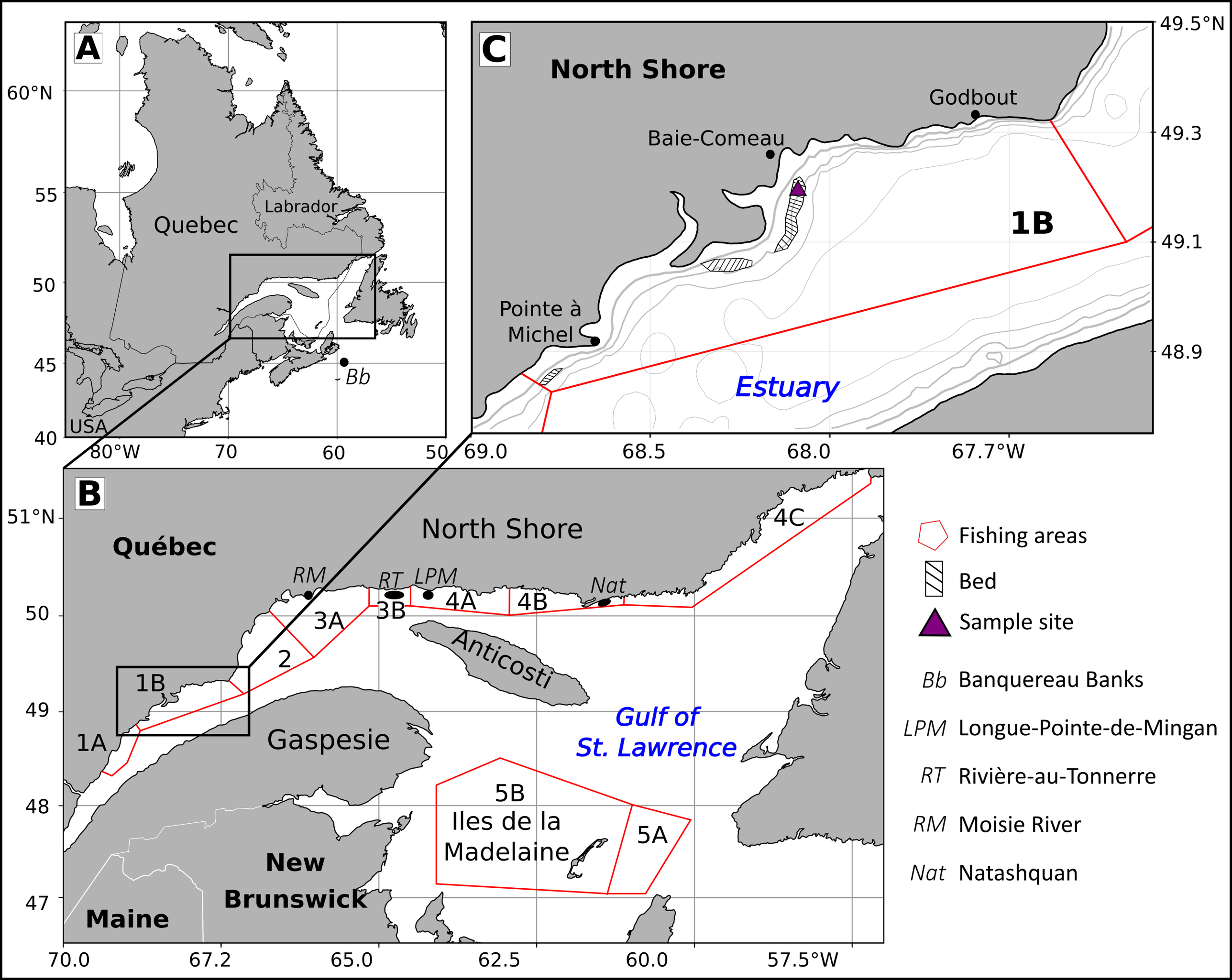
A
60°N
55
50
45
40
80°W
70
60
50
Quebec
Labrador
Bb
USA
C
North Shore
Godbout
Baie-Comeau
1B
Pointe à
Michel
Estuary
49.5°N
49.3
49.1
48.9
69.0
68.5
68.0
67.7°W
B
51°N
50
49
48
47
70.0
67.2
65.0
62.5
60.0
57.5°W
Québec
North Shore
RM
RT
LPM
Nat
4C
4A
4B
3A
3B
2
1B
1A
Anticosti
Gaspesie
Gulf of
St. Lawrence
5B
Iles de la
Madelaine
5A
New
Brunswick
Maine
Fishing areas
Bed
Sample site
Bb Banquereau Banks
LPM Longue-Pointe-de-Mingan
RT Rivière-au-Tonnerre
RM Moisie River
Nat Natashquan

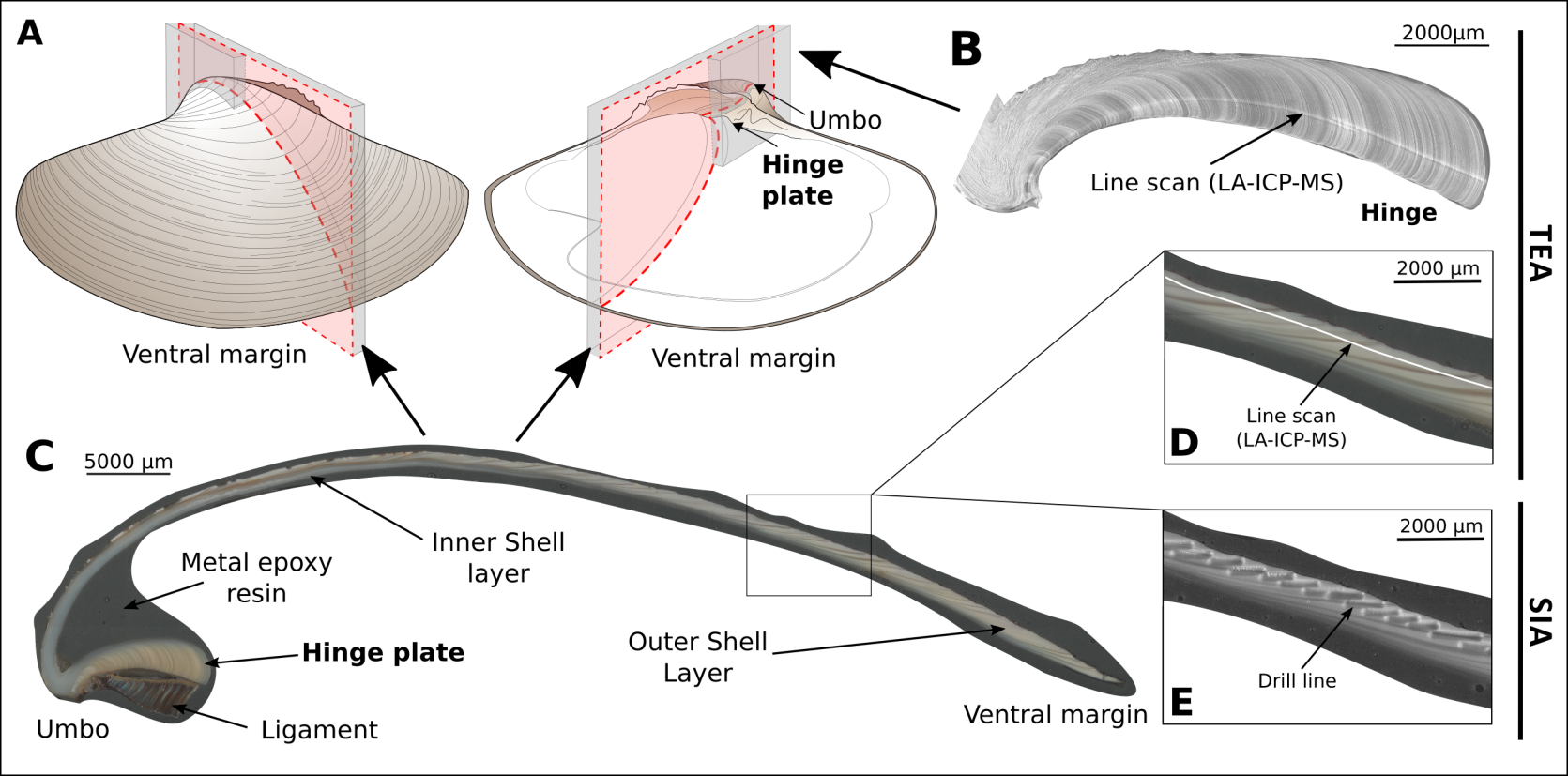
A
Ventral margin
Umbo
Hinge plate
Ventral margin
B
2000µm
Line scan (LA-ICP-MS)
Hinge
TEA
2000 µm
Line scan (LA-ICP-MS)
D
C
5000 µm
Inner Shell layer
Metal epoxy resin
Hinge plate
Umbo
Ligament
Outer Shell Layer
Ventral margin
2000 µm
Drill line
E
SIA

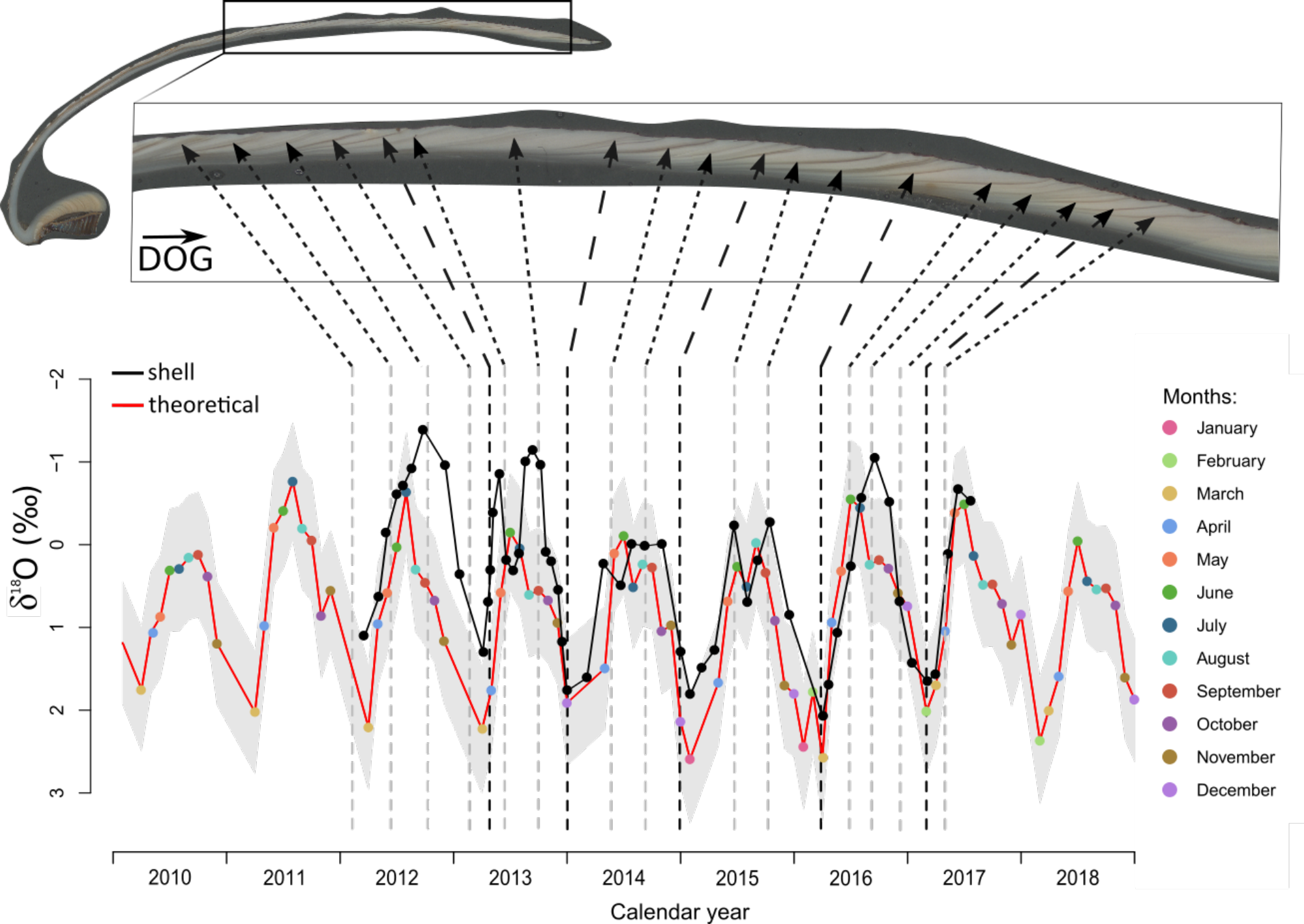
DOG
shell
theoretical
$\delta^{18}O$ (‰)
−2
−1
0
1
2
3
Months:
January
February
March
April
May
June
July
August
September
October
November
December
2010
2011
2012
2013
2014
2015
2016
2017
2018
Calendar year

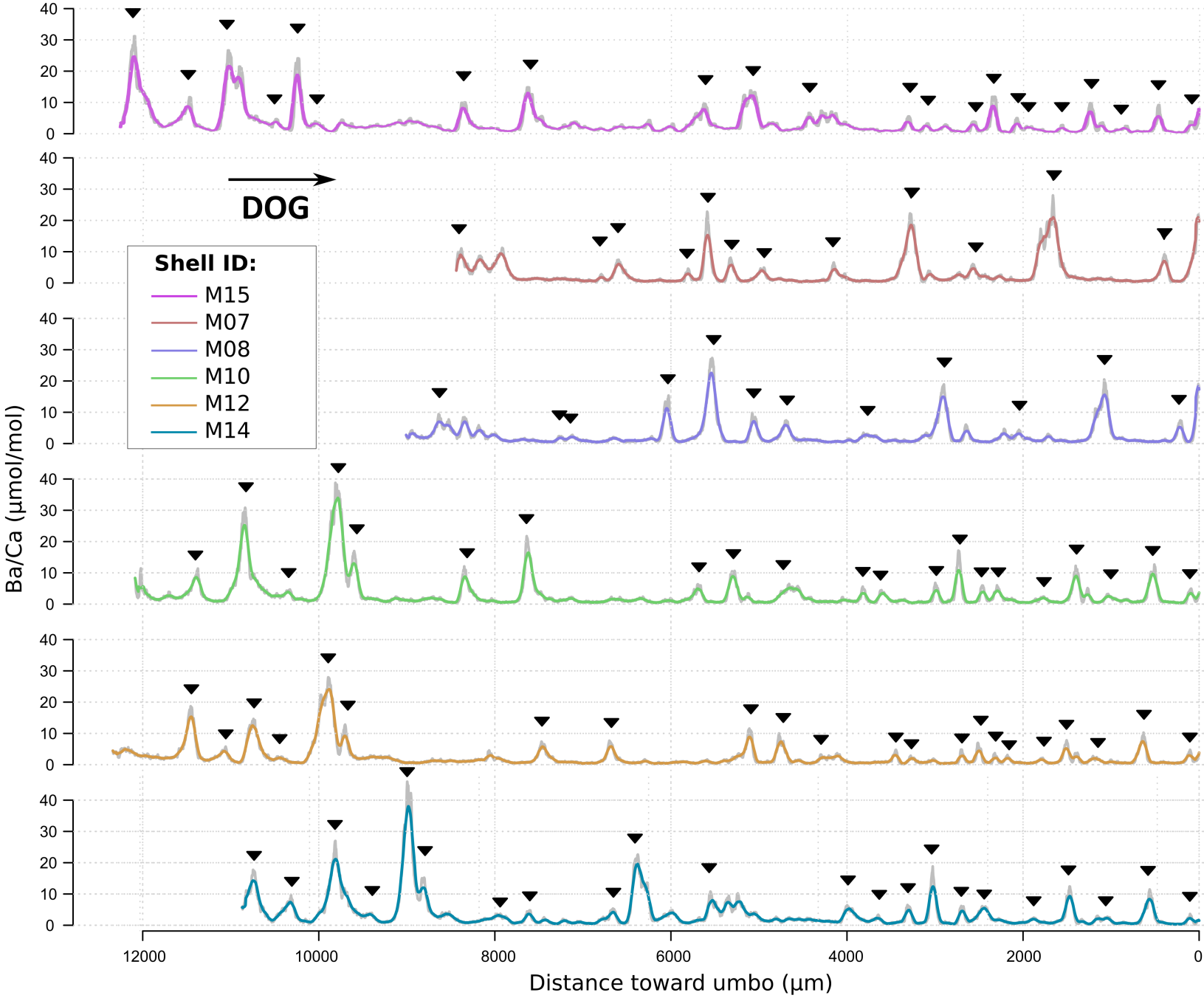
DOG
Shell ID:
M15
M07
M08
M10
M12
M14
Ba/Ca (µmol/mol)
Distance toward umbo (µm)
0
10
20
30
40
12000
10000
8000
6000
4000
2000
0

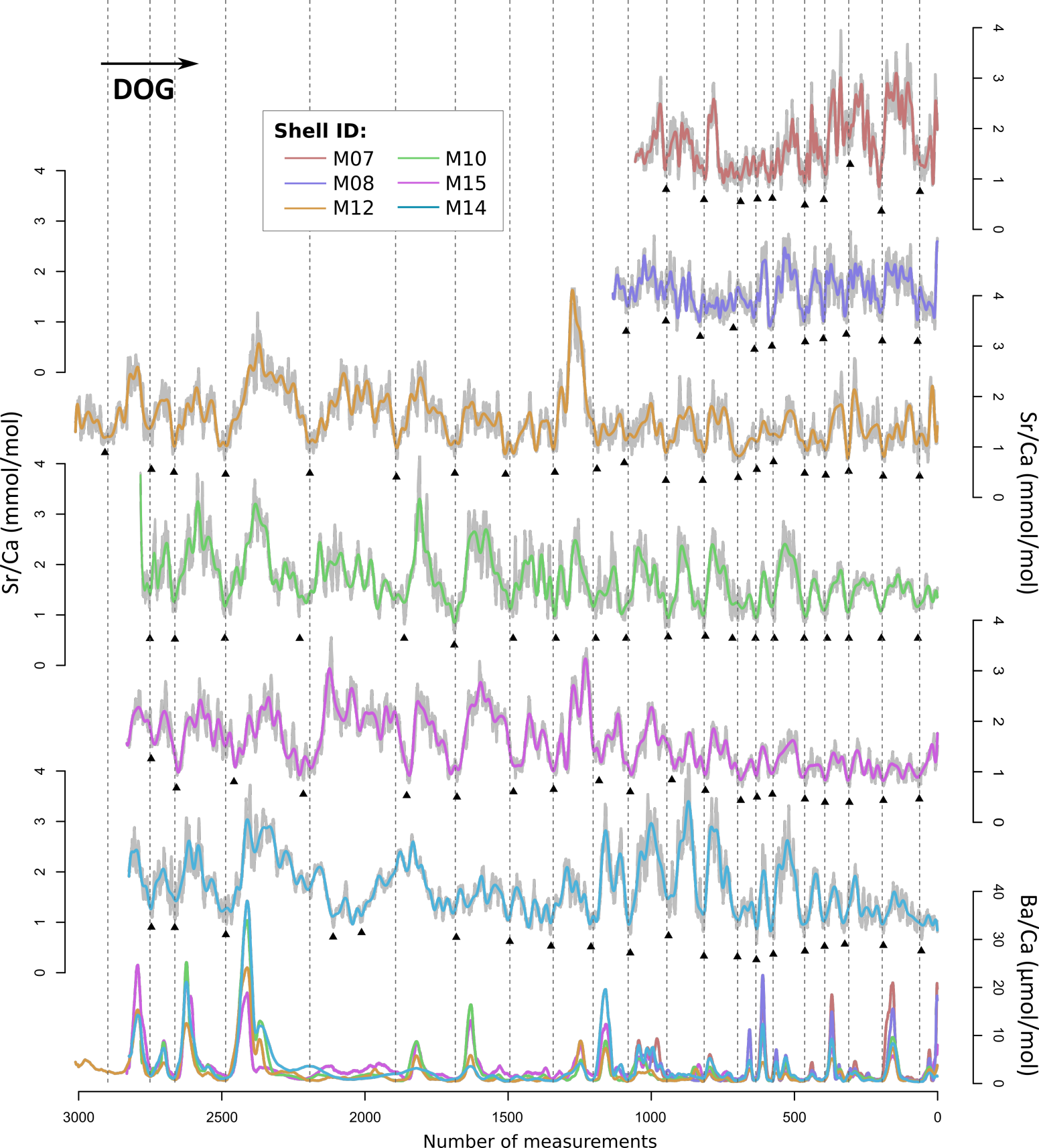
DOG
Shell ID:
M07
M08
M12
M10
M15
M14
Sr/Ca (mmol/mol)
Sr/Ca (mmol/mol)
Ba/Ca (µmol/mol)
Number of measurements
3000
2500
2000
1500
1000
500
0

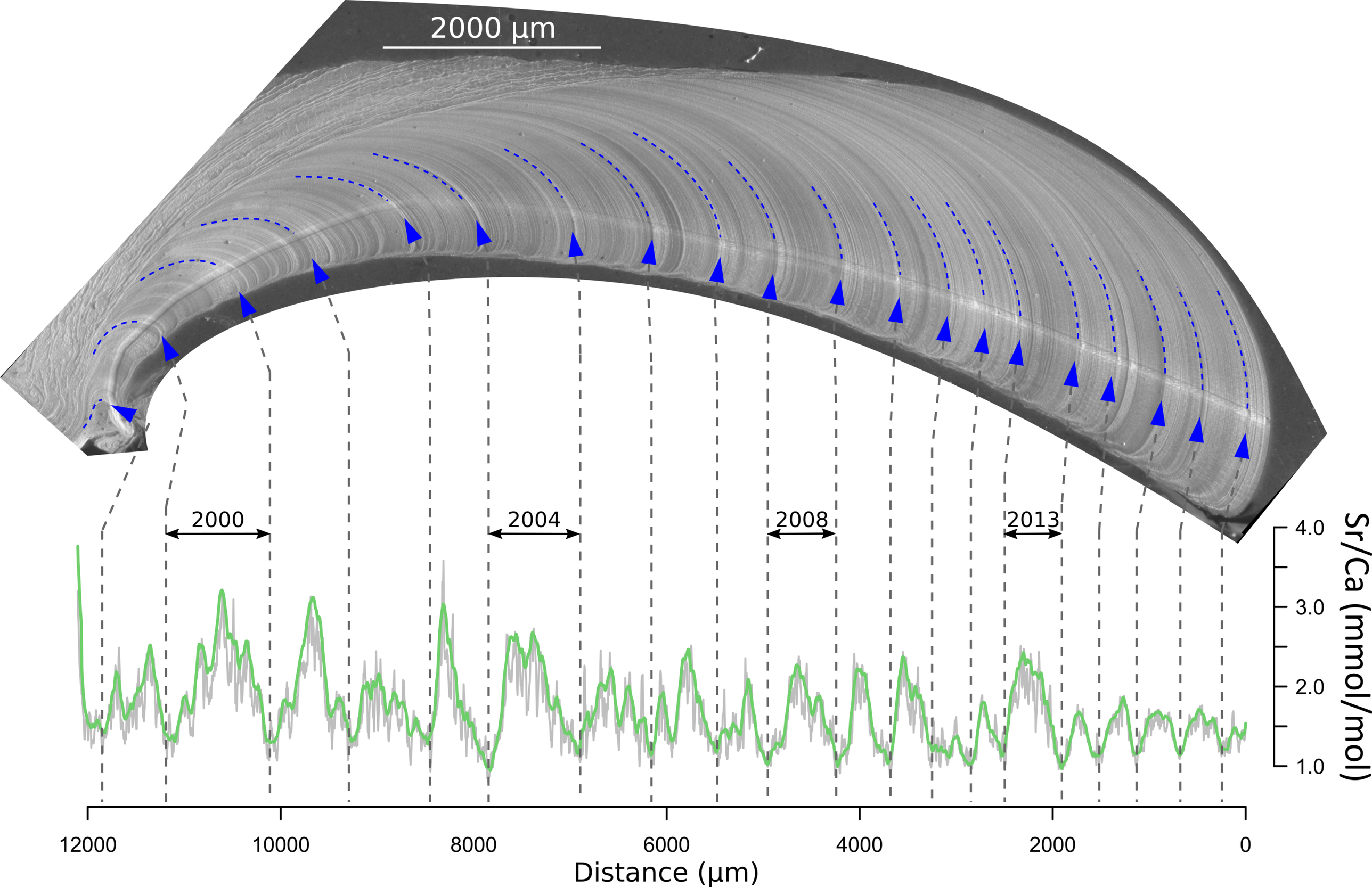
2000 µm
2000
2004
2008
2013
4.0
3.0
2.0
1.0
Sr/Ca (mmol/mol)
12000
10000
8000
6000
4000
2000
0
Distance (µm)

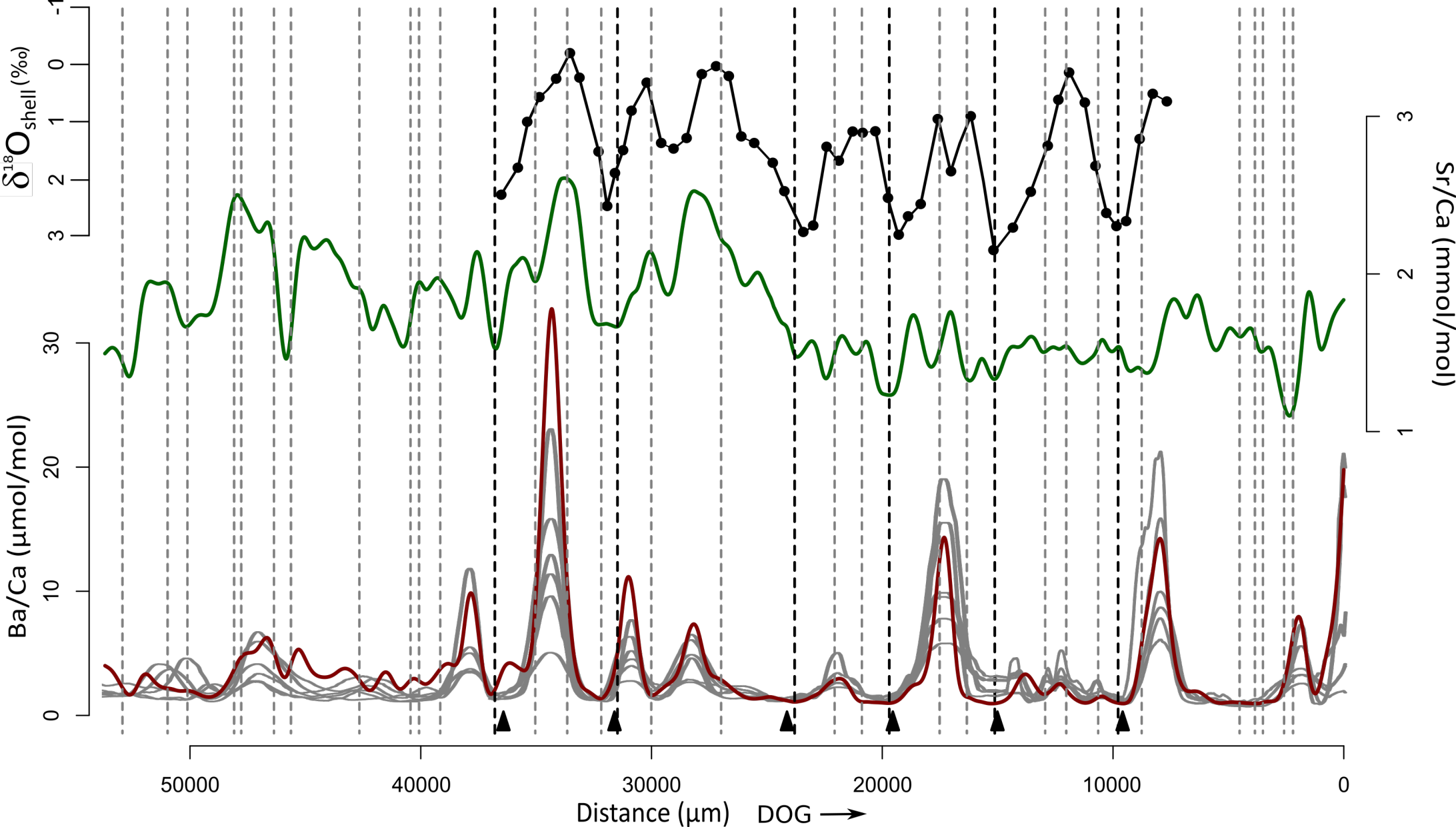
δ18Oshell (‰)
-1
0
1
2
3
Sr/Ca (mmol/mol)
1
2
3
Ba/Ca (µmol/mol)
0
10
20
30
50000
40000
30000
20000
10000
0
Distance (µm)
DOG

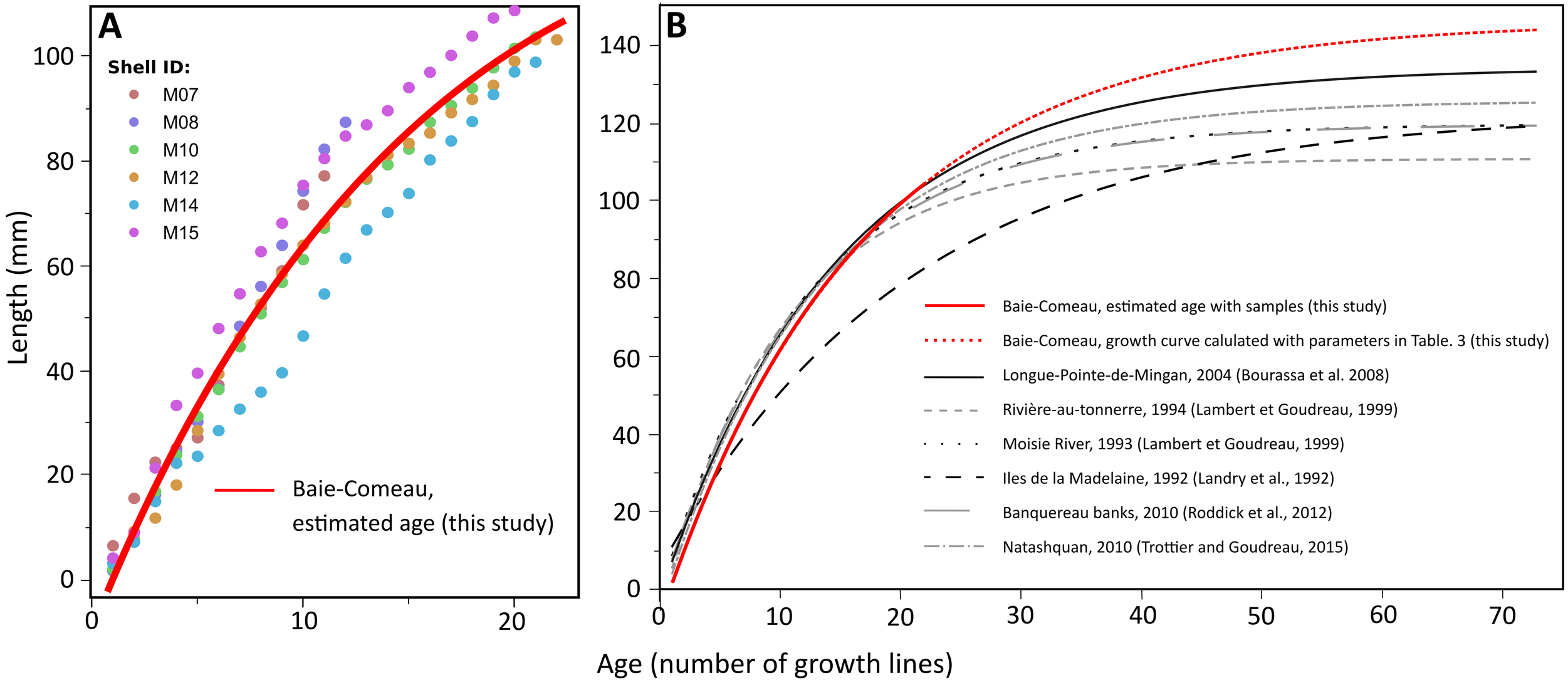
A
Shell ID:
M07
M08
M10
M12
M14
M15
Baie-Comeau,
estimated age (this study)
Length (mm)
0
20
40
60
80
100
0
10
20
B
Baie-Comeau, estimated age with samples (this study)
Baie-Comeau, growth curve calulated with parameters in Table. 3 (this study)
Longue-Pointe-de-Mingan, 2004 (Bourassa et al. 2008)
Rivière-au-tonnerre, 1994 (Lambert et Goudreau, 1999)
Moisie River, 1993 (Lambert et Goudreau, 1999)
Iles de la Madelaine, 1992 (Landry et al., 1992)
Banquereau banks, 2010 (Roddick et al., 2012)
Natashquan, 2010 (Trottier and Goudreau, 2015)
0
20
40
60
80
100
120
140
0
10
20
30
40
50
60
70
Age (number of growth lines)

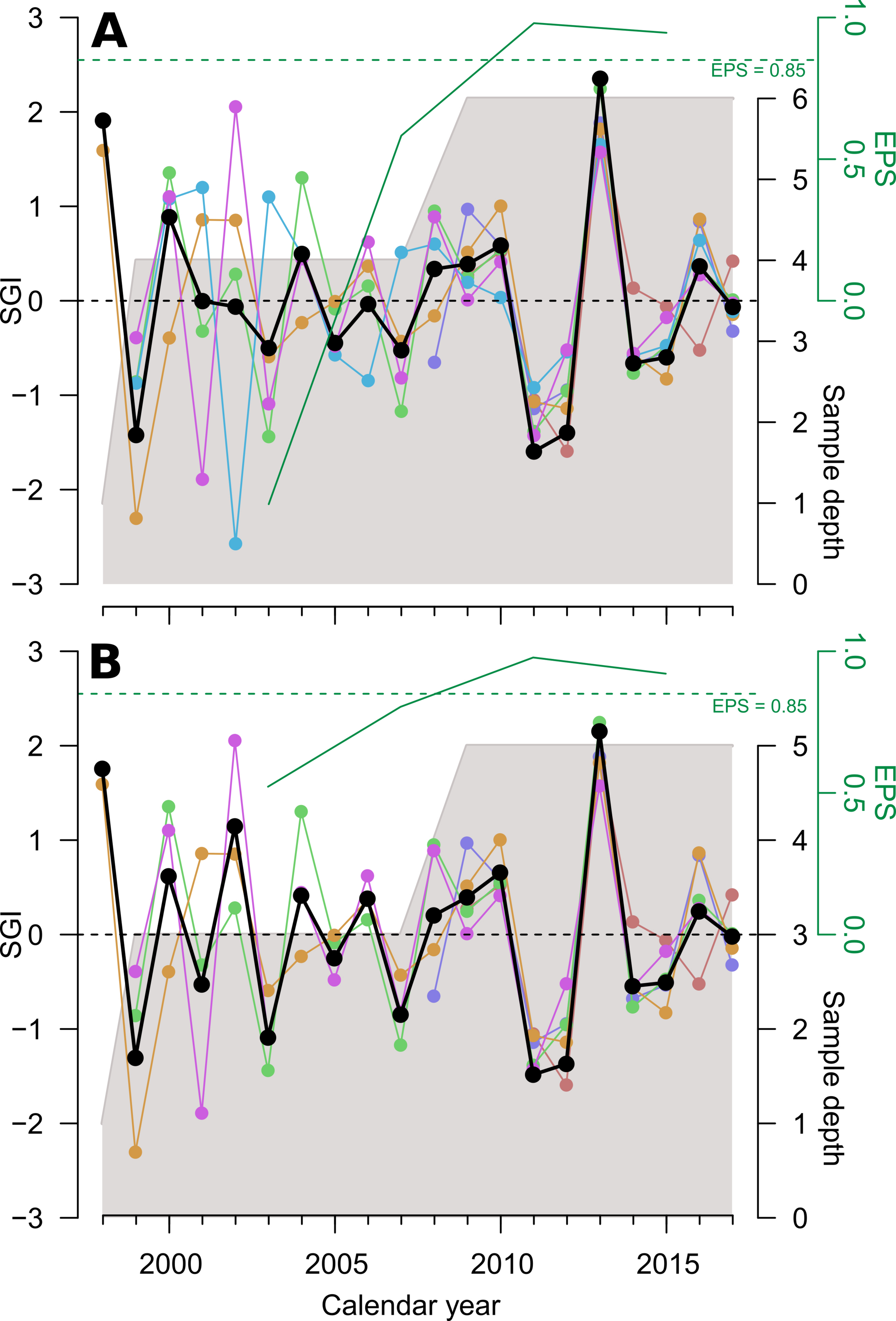
A
B
EPS = 0.85
SGI
Sample depth
EPS
Calendar year
2000
2005
2010
2015